Mestrado Integrado em Engenharia Química

NO$_X$ Assisted High Temperature Soot Oxidation

Screening of the catalytic systems based on high-surface area ZrO$_2$ as support

Tese de Mestrado

desenvolvida no âmbito da disciplina de

Projecto de Desenvolvimento em Instituição Estrangeira

Bruno Barrias

Delft University of Technology

Universidade do Porto
Faculdade de Engenharia
FEUP

Departamento de Engenharia Química

Orientador na FEUP: **Prof. José Figueiredo**
Orientador no estrangeiro: **Dr. Arkady Kustov**
Dr. Ir. Michiel Makkee

Julho de 2008

Abstract

Abatement technologies for soot and NO_X have become a topic of relevant research over the years due to the stricter legislations. Oxidation-based technologies may be a useful solution to reduce soot by converting it to CO_2. However, high temperatures are needed. As a result, catalysts that promote soot combustion at lower temperatures are required. Since soot oxidation by O_2 requires temperatures above 600°C to start uncatalysed soot oxidation, the possible solution is to use NO_2, which is a better oxidant.

Soot can be collected by placing a filter device in the exhaust line. But the problem is that the filter has to be periodically or continuously regenerated, for example by oxidation of carbon in CO_2. In this work we study active regeneration that uses NO_2 as oxidant by using a catalyst that combine a NO_X storage material and oxidation catalyst. This material will store the NO_X at temperatures below 300°C as nitrates and release it at the temperature range of regeneration (500-600°C). An oxidation catalyst increases the efficiency of the system.

For this purpose a model NO_X storage system 20% $MeNO_3$ supported on ZrO_2 (90 m^2/g), where Me = Mg, Ca, Sr, Ba (alkaline earth metals) and La, Ce, Pr (rare-earth metals) and Pt as oxidant was prepared. This support was chosen because earth metals and ZrO_2 are known to form nitrates upon reaction with NO_X.

Textural properties of the catalytic systems were studied by TGA. NO_X storage/release cycles were analyzed by FTIR-MS and TPD-MS. Soot oxidation was studied by TPD-MS and six-flow reactor. It was used loose contact mixtures between the soot and catalysts.

It was found that introducing stored nitrates into the system decrease the temperature of soot oxidation more than 70°C in comparison with uncatalysed soot oxidation. The best storage capacity was achieved for Ca and Sr-based systems, 91% and 61% respectively in TPD-MS. The combination of bulk nitrates and platinum increases soot oxidation, as well as the selectivity of soot conversion to CO_2. It was stated that platinum has almost no effect on NO_X storage capacity but can decrease the temperature of nitrates decomposition/desorption.

Sr based-system was chosen as the final catalyst to optimize in terms of NO_X storage and soot oxidation performance. It was found that pretreating the catalyst in reducing atmosphere (air + 5% H_2 in argon), storage capacity increase to more than 85% and the amount of NO_X desorbed between 200 and 500°C also increased. Different activation procedures were used. The best results were achieved by the "standard" method. Good stability was obtained. ZrO_2 supported system follows the same trend as for Al_2O_3 system. However, zirconia support can store more nitrates.

Acknowledgements

In first place I would like to say that was a pleasure doing Erasmus in Netherlands, especially in the Catalysis Engineering group. I would like to thank Dr. Ir. Michiel Makkee for all the knowledge that he pass me through during all the meetings that we have and all the guidance through out the project. Furthermore, I'm thankful to my daily supervisor Dr. Arkady Kustov for his help during my thesis. For making a better engineer than when I started my project. Thank you very much for your advices and patience.

I would like to express my gratitude to the technical assistance: Bart for helping every time I needed, solving all kind of problems in the TPD-MS and FTIR-MS set up; Harrie for helping me with six-flow reactor set-up and experiments and Sander Brower for all the technical support in the TPD-MS. I should say that during the entire process I was very impressed with the quality and cooperation of the technicians.

I like to thank also my nice "office mates" sitting in 0.456: Francesca, Delphine, Nicla, Marco, Martijn, Maarten, Michiel and Ugur. It was real fun all our discussions about football, dutch food and costumes and dialogues about all the aspects of our life. Special thanks to the Catalysis Group, in particular the Portuguese community - Joana, Rita, Alexandre and Patrick.

Many thanks to Andrea for the good italian atmosphere and for his friendship. I would also like to thanks my friends back in Portugal, although so far I felt them closed to me, especially thanks to Ticas, Tiago and Patricia for their never-ending friendship.

Countless thanks to Claudia, my love, for all the moments that I pass with you in the Netherlands, for all the understanding and patience with me. I really enjoy all that we been through. Jose and Eva for encouraging and support during my staying in Holland.
To my Brother Hugo for all the laughs that he provides and help I needed.

For last to my dear parents, Fernando and Anabela for always support me during my life. They are responsible for the man I am. They created solid roots from which I grew and became a good person. Thanks for the good education and the help for realizing my dreams.

Table of Contents

Index of Figures

Index of Tables

1. Introduction

Air contains numerous particles originating from natural and synthetic materials, as found in wildfires and combustion processes. The human pulmonary system can resist against larger particles but not against particles smaller than 10 μm (designated as PM-10). As a response new research efforts have been made to evaluate the health effects that these smaller-size particles have, especially for cases of diesel particulate matter (PM) [1].

Diesel engine exhaust gases contribute significantly to urban and global air pollution. Emissions of hydrocarbon (HC) and CO from diesel exhaust gases are low and can be easily converted by using diesel oxidation catalyst (DOC). However, even the most recent diesel engines generate nitrous oxides (NO_X) and carcinogenic particulates, whose size range of 50–200 nm falls in the dangerous range. These particles consist of carbonaceous soot that carries many toxic compounds, such as poly-aromatic hydrocarbons (PAH). Further improvements in modern diesel engine design and combustion process will ideally lead to decreased amounts of NO_X (NO + NO_2, though mainly present as NO) and particulate (carbon soot) emissions. Even these improvements in diesel fuel engines and combustion processes alone cannot meet the targets set in recent legislation from Europe (in the agendas known as Euro 5 and 6) for NO_X and soot. Therefore, abatement technologies for soot and NO_X have become a topic of relevant research. Oxidation and reduction-based technologies may be a useful solution to reduce soot and NO_X amount by converting them to the better managed CO_2 and N_2, respectively.

However, during typical diesel engine operations, the exhaust gas temperature is below 300°C, but that temperature is too low to operate continuous un-catalysed soot oxidation that occurs around 600°C [1] [2]. Therefore, catalysis is required to lower the temperature of soot oxidation. To support the oxidation process, a filter collects soot particulates in the exhaust gas and periodically converts them to CO_2. Two filter schemes are currently used to convert soot, classified as passive and active filter regeneration strategies. Passive regeneration can be applied on heavy duty diesel vehicles, such as trucks and buses, because the engine often works within an exhaust temperature range of 250–400°C. However, this scheme cannot be applied to light duty vehicles, since the exhaust temperatures of diesel passenger cars rarely exceed 250°C. The advantage of active systems is that they will function effectively even if the desired exhaust temperatures are not achieved in normal operation and consequently can be employed in vehicles/equipment with low exhaust temperatures.

Soot oxidation by O_2 occurs at a significant rate above 550 °C. The temperature inside the DPF (diesel particulate filter) is lower (200–450 °C) under normal driving conditions. Therefore catalysts that promote soot combustion at lower temperatures are required. Active regeneration with NO storage materials is a possible solution.

NO_2 has a better oxidative capability than O_2, so the possible utilization for the filter is to use NO_X storage material which will store the NO_X at temperatures below 300°C as nitrates and release it at the temperature of regeneration via reversed reactions. In this case, the efficiency can be improved further if we add oxidation catalysts which will oxidize NO into NO_2 and later converts soot selectively into CO_2 and back to NO which can participate in the next soot oxidation event. Because of the decreasing amounts of NO_2 at higher temperatures the main role of oxidation catalyst is to provide the recycling of NO to NO_2 with high efficiency. Several catalysts have been reported, particularly the Pt/Al_2O_3, $Pt/K–Al_2O_3$, $Pt/Ba–Al_2O_3$ [3] and also $Co,Ba,K/CeO_2$ [4]. However, only a part of the stored NO_X that is decomposed at high temperatures under lean conditions is found to be useful for soot oxidation. NO_X storage capacity decreases upon ageing under soot oxidising conditions. This will lead to a decreased soot oxidation activity on stored nitrate decomposition. $Pt/K–Al_2O_3$ catalyst is more active and more stable compared with $Pt/Ba–Al_2O_3$.

The increased interest in particulate filter regeneration systems and the promising results of NO_2-assisted systems have motivated research over the years [5] [6]. Nevertheless, due to the high commercial interest of these systems, there are few published works, and most of them only study reaction rates at *laboratory* scale using *synthetic* soot. Therefore, in this work, we will study the capability of a material that will store the NO_X at temperatures below 300°C as nitrates and release it at the temperature range of regeneration. If we add an oxidation catalyst the efficiency can be improved because the oxidation rate of soot and the recycling of NO to NO_2 are increased.

2. Literature Review

2.1 Diesel engine and emissions

Gasoline and diesel engines are the most common combustion engines used in the world. During the combustion of fuel in these engines several undesirable by-products are formed that can be dangerous for human health, particularly from diesel combustion.

As a result of the growing urbanization and the exhaust gas emissions, serious threat to air quality emerge, leading to the first legislation standard in 1970. Along the years standards were tightened, and as a result catalytic converters (Figure 1) became necessary. Nowadays, every car

is equipped with a catalytic converter, reducing CO, HC, and NO_X, emissions typically by 80-95%. The first generation of catalytic converters used in diesel emission control were the "flow through monoliths". These monoliths had been used in TWC (three way catalysts) in gasoline exhaust since the first emission regulation was enacted. These monolithic ceramic filters have open channels covered with a high surface area wash-coat (Al_2O_3 or SiO_2) on which a small amount of precious metal (Pt or Pd) is coated [1].
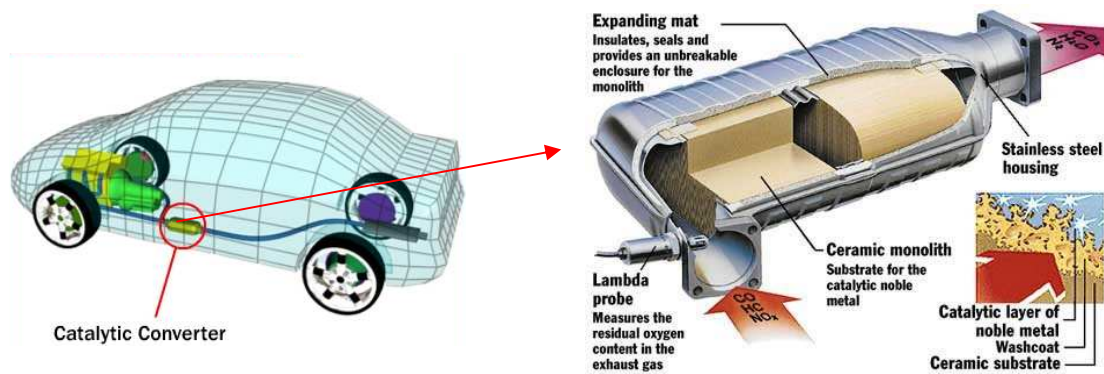
Figure 1 – Schematic representation of a catalytic converter (example: three way catalyst) [7].

The three way catalysts (TWC) are described in the literature as the best catalytic converters, and are called that way because all three pollutants (NO_X, CO and HC) are removed from the exhaust gas simultaneously. However, this type of catalysts "works" with very low or none oxygen content, so in that case can be applied only to gasoline engines, which have stoichiometric air to fuel ratios. After the successful introduction of three-way catalysts the attitude towards diesel engine emissions were influenced, because they had always been considered clean in comparison with gasoline exhaust gases. Today, CO and HC emissions from modern gasoline engines are similar to diesel engines. Nevertheless, the NO_X, and certainly the particulate emissions from diesel engines are much higher. Particulate standards for diesel engines were introduced in 1992 [8]. In Europe diesel vehicles are responsible for 43% and 72% of NO_X and PM (particulate matter) emissions respectively, of the "on road" emissions [9]. Therefore, they represent negative impact on our health and in the environment. As a result it is very important to decrease these emissions.

Nowadays the diesel engines are well spread across the world because of lower fuel prices (partly because of less severe tax levels), durability, low maintenance requirements and large indifference to fuel specification. In Europe 100% of heavy-duty, 60% of light commercial vehicles, and 20% of passenger cars are diesel-powered [10].

In diesel engines fuel is injected after the air is compressed in the combustion chamber causing the fuel to self ignite. The air-to-fuel ratio λ (which is defined as the ratio of air available to air required for complete combustion), varies between 1.1 and 6. The diesel internal combustion engine differs from the gasoline because uses a higher compression (16-24) of the

fuel to ignite the fuel rather than using a spark plug ("compression ignition" rather than "spark ignition").

In gasoline engines, air and fuel are pre-mixed before compression. The air-to-fuel ratio is constant and is often chosen to be stoichiometric. The mixture is compressed in the cylinder and ignited by a spark plug. Pre-mixing of fuel and air severely limits the compression (6-10), and thus efficiency. Fuel efficiency for a diesel engine is 30-50% higher than that for a gasoline engine with comparable power. The difference in the efficiency is caused by: energy losses at the throttle valve; differences in compression ratio and differences in air-to-fuel ratio (higher O_2 concentration in the diesel combustion chambers) [8]. These differences are responsible for the better fuel efficiency. In addition, diesel fuel has approximately 15% more energy per unit volume than gasoline. Therefore, when compared on a miles per gallon basis, diesel engines begin with a 15% advantage over gasoline engines. In the following table are the compositions of exhaust gases emitted from diesel and gasoline engines (lower value can be found in new clean engines while the higher numbers are characteristic for older engines).

Table 1-Typical compositions of the diesel and gasoline exhaust for passenger cars (M_1)[10-12].

	CO (g/km)	HC (g/km)	NO_X (g/km)	PM (g/km)	Exhaust Temperature (K)	Exhaust flow-rate (m^3/h)
Diesel	0.5-1.0	0.40-0.60	0.20-2.0	0.01-0.2	373-635	40-50
Gasoline	1.0-6.0	0.40-0.60	0.10-0.80	0.005-0.01	573-750	30-40

Carbon monoxide (CO), hydrocarbons (HC), sulphur dioxide (SO_2), nitrogen monoxide and nitrogen dioxide (NO_X) and particulates (PM), also called soot are subject to legislation, which will be discussed further in section 2.1.2.

2.1.1 Environment and health effect of diesel emissions

As previous mentioned the diesel engine exhaust emits severe pollutants, which can pose serious public health concerns, particularly particulate matter (soot). In the urban areas, where exposure to diesel exhaust may be especially high, soot becomes a bigger problem. In general, particles inhaled by humans are segregated by size during deposition within the respiratory system. Larger particles deposit in the upper respiratory tract, while smaller particulate denominated PM-10 (particulates smaller than 10 μm) travels deeper into the lungs and retained for longer periods of time, which may cause adverse health effects, like asthma and increase the probability of lung cancer and the risk of premature death. If the smaller particles are present in

greater numbers, they have greater total surface area than large particle of the same mass, so they are more likely to interact with cells in the lung than those carried by larger particles. Also these smaller particles contain a quantity of organic materials, such as polynuclear aromatic hydrocarbons (PAH), alkylated benzenes, which might have significant long-term health effects. In fact several of them have shown carcinogenicity and mutagenicity [13].

2.1.2 Diesel emissions legislation

The growing awareness of the effects of pollutants on the environment and human health has made legislation on the emission of, among others, diesel-powered vehicles more and more stringent over the years. European Union emission regulations for new light duty vehicles (cars and light commercial vehicles) are specified in the Directive 70/220/EEC.

Since the Euro 2 stage, EU regulations introduce different emission limits for diesel and gasoline vehicles. Euro 5/6 regulations have stricter emission for NO_X and PM, since it adopts a new PM mass emission measurement method developed by the UN/ECE Particulate Measurement Programme (PMP). PMP method introduces a particle number emission limit, in addition to the mass-based limits. Number-based PM limits would prevent the possibility that in the future open filters are developed that meet the PM mass limit but enable a high number of ultra fine particles to pass [14]. As an example, diesel emission standards for passenger cars (vehicle categories M_1) are summarized in Table 2. For the sake of brevity the standards for the other categories are not covered here.

Table 2 - EU diesel emissions standards for passenger cars (Category M_1), g/km [14].

Tier	Date	CO	HC+NO_X	NOx	PM
Euro 1	7/1992	2.72	0.97	-	0.14
Euro 1, IDI	1/1996	1.0	0.7	-	0.08
Euro 2, DI	1/1996	1.0	0.9	-	0.10
Euro 3	1/2000	0.64	0.56	0.5	0.05
Euro 4	1/2005	0.50	0.30	0.25	0.025
Euro 5	9/2009	0.50	0.23	0.18	0.005 [a]
Euro 6	9/2014	0.50	0.17	0.08	0.005 [a]

[a] - proposed to be changed to 0.003 g/km using the PMP measurement procedure

In addition to complying with the emission limits mentioned above, for the Euro 5/6 vehicle manufacturers must also ensure that devices fitted to control pollution are able to last for a distance of 160 000 km or 5 years (whichever occurs first).

The Euro 4 requirements could be fulfilled without further exhaust gas treatment, but for Euro 5 the manufacturers will require the use particulate filters. Given this progress, the diesel car will soon be ''seen'' as a much more environmentally friendly vehicle than it was previously.

2.2 The characteristics of diesel particulate matter

Various terms are used to describe the particles emitted by diesel engines. Often this lead to confusion, however we can call diesel particles to the individual particles present in the exhaust gas. The diesel soot is the carbonaceous part of diesel particulate matter (PM). It is the fraction that is oxidized during regeneration of a diesel particle filter.

The carbonaceous soot is formed in the centre of the fuel spray droplets, where the air/fuel ratio is low. Non-ideal mixing of fuel and air creates pockets of excess fuel, where solid carbonaceous soot particles (the solid and the soluble organic fraction, SOF) are formed [15].

A scheme of the diesel exhaust particles size and distribution, and the schematic structure and composition of a typical diesel particulate system are shown in Figure 2.

a)   b)
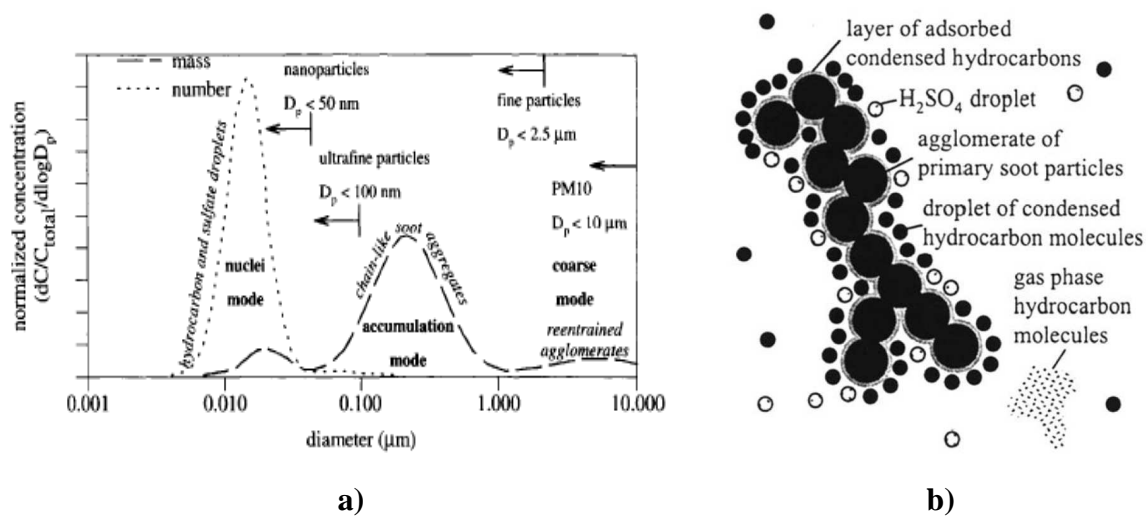
Figure 2- **a)** Scheme of engine exhaust particle size distribution, both mass and number based concentration; **b)** Schematic representation of diesel soot and its adsorbed species. After [1].

The soot particles consist of a carbonaceous solid core with adsorbed hydrocarbons, sulphates, nitrates, metals, water and some trace compounds, such as, polycyclic aromatic hydrocarbons (PAH) that are very harmful for health, as was previous mentioned. The PM is typically composed of 50% to 75% elemental carbon (EC). The particles tend to agglomerate because adsorbed hydrocarbons, sulphate, and water act as "glue", increasing the particle size and mass distribution to what is observed in **b)** [16]. The size of individual soot spheres is about 25 nm, while the size of total particulates is about 200nm [16].

Due to the stricter legislation over the years and the danger of these particulates, strategies for reducing the diesel exhaust emissions were initiated.

2.3 Strategies in diesel emissions control

For a diesel engine the emissions of particulate matter and NO_X have an inverse correlation. An effort to reduce soot particles is always associated with an increase in NO_X. The emissions of CO and HC can be treated very easily with a noble metal oxidation catalyst, like the Diesel Oxidation Catalyst (DOC), but for the removal of NO_X and PM from diesel engines the task is more difficult. There are several strategies to reduce emissions from diesel engines, like engine modification, fuel reformulation, and exhaust after-treatment system.

Modifying the engine reduces NO_X emissions via Exhaust Gas Recirculation (EGR), HC post injection and water injection, but has also several drawbacks [12,17,18]. The particulate matter can be reduced by retarding injection of the fuel, increasing the injection pressures or by turbo charging [8]. A small reduction of diesel regulated emissions can be achieved by modifications in diesel fuels using lower sulphur contents, but is not enough to meet the minimal requirements.

Besides engine adjustment and fuel reformulation, after-treatment techniques can be used to reduce the NO_X and PM emissions. The reduction of the NO_X cannot be applied to the conventional technology (three-way catalyst) because diesel engines operate with more air than needed for the combustion process (lean burn). There are 2 main options for the NO_X after-treatment: selective catalytic reduction (SCR) with HC, NH_3 or urea, and NO_X storage reduction (NSR) catalyst [15] often also called lean-NO_X trap (LNT) catalysts [18,19], that will be further discussed in section 2.4.3.

Engine adjustment and fuel reformulation have greatly contributed to the reduction of PM emission. The suppression of lubricant oil combustion and the fuel quality like, fuel density, cetane number, sulfur-, oxygen- and aromatics content resulted in a substantial reduction of particulate emission [18]. However, it is anticipated that particulate reduction via engine modification and fuel reformulation will not meet future standards. For that reason, in the future after-treatment techniques have to be used. There are two ways: the catalyst is added to the fuel (fuel borne catalyst) or coated on a filter.

. Fuel borne catalysts are blended into the fuel and therefore can act with the structure of the soot. Thus, the catalyst-soot contact, which is crucial for solid-solid reactions, is increased. The most commonly used fuel additives are Ce and Fe [4]. However, the blending of the catalysts in the fuel can be a problem and the additive can be retained within the filter. Nevertheless, PSA

Peugeot Citroën uses since 1999 a particulate filter system with a fuel additive system integrated (Ce and Fe-based catalyst additive is used) with success.

The second alternative is the catalyst coated on the filter's surface. This way the filter collects the soot particles and acts as a substrate for the catalyst. The reaction takes place on the filter's surface, and the catalyst – soot contact attained is a little worse than that of the fuel borne catalysts. However, this way the problem of catalyst consumption is prevented and extra cost of using a separate system for catalyst blending and storage is avoided [20].

Thus, the use of a filter is the most straightforward method for reducing particulate emissions. There are several types of filter, such as, wall-flow monolith filter, ceramic foams, candle filters, metal wool filters and wire mesh filters. The general term for filters which remove particulates from diesel exhaust gases is "particulate trap". Unmistakably the most studied and applied particulate trap is the wall-flow monolith because of the easiness to use, large scale production and good collection efficiency (90-95%). Figure 3 [21] shows a typical wall-flow monolith filter commonly used as a particulate trap.
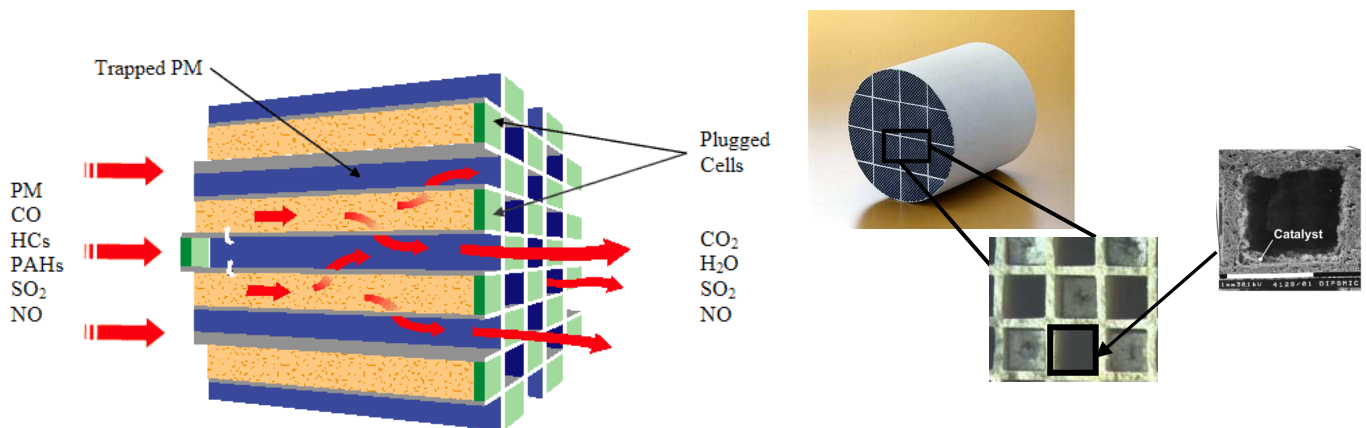
Figure 3 – Several schematic representations of wall-flow monolith.

It consists of ceramic structure with parallel channels of which half are closed in an alternate checker board manner from upstream side and other half are closed at the downstream end. Therefore the exhaust gas cannot flow directly through a given channel. It enters the upstream side of the trap where the channels are open (inlet channel), forced through the porous walls of the channels to exit through the adjacent channels where the ends are open (outlet channel). As a result, exhaust gases are forced to flow through the porous walls, which then act as filters, in this way high particulate trapping efficiency can be achieved. If too much PM accumulates , the back-pressure across the filter will increase and degrade engine performance, and ultimately the engine will cease to function [16].

Still, when using a particulate trap, a regeneration technique is necessary, from time to time, to prevent the trap becoming clogged with collected soot which, in the longer term, would result

in engine malfunction due to increased back-pressure. Several techniques for removing particulates from the filter have been proposed.

The easiest one is the non-catalytic regeneration. In this case, the temperature is increased to initiate fuel combustion by air which is present in the exhaust. This method is relatively simple and has the advantage of not needing a catalyst, but requires temperatures above 600°C. This type of regeneration can easily get out of control and damage the filter due to chaotic thermal runaways. Another problem is the low regeneration efficiency: up to 35% of the soot can be retained in the filter creating soot gradient build-up [4].

As an alternative, the use of catalysts for soot removal from particulate traps seems to be a logical choice, since catalysts for oxidation of carbonaceous materials have been studied for a long time. But in fact it is not that easy, since both soot and particulate trap are solid, and there is a big problem of the contact between them. There are two approaches to overcome this problem: passive regeneration or active regeneration.

Passive regeneration is commonly based on the fact that NO_2 is a more powerful oxidant than oxygen and it is present as a component of exhaust gases and in this way the filter can regenerate in normal vehicle/equipment operation without any additional assistance. Therefore, soot can be continuously and effectively oxidized at much lower temperatures. However, oxidation of soot with NO_2 requires relatively high temperatures and high NO concentrations in exhaust gases, therefore it can only be used in heavy duty diesel vehicles because the engine often works at high load and the exhaust temperature is in the range 250–400°C (CRT system) [22], while diesel passenger cars rarely exceed 250°C in city driving. The advantages of passive systems are: technology less complex, require far less servicing, and are less expensive than active systems. Examples of passive diesel particulate filters (DPF) are filters coated with a catalytic material, a diesel oxidation catalyst upstream of the DPF, and a FBC (fuel borne catalyst) used in combination of a filter.

When passive regeneration is not possible the system needs to be subjected to active regeneration. In this case, the temperature is raised periodically to combust accumulated soot. But unlike non-catalytic regeneration, a catalyst can be used to increase the efficiency of soot combustion. The advantage of active systems is that they will function effectively even if the desired exhaust temperatures are not achieved in normal operation and consequently can be employed in applications on which passive filters cannot be used. An active DPF system relies on additional strategies to ensure that filter regeneration occurs. For active regeneration it is possible to take advantage of NO storage materials.

As previously mentioned, catalysts seem to be the best solution for oxidizing soot. For that reason, catalytic soot oxidation has been studied over the years.

2.4 Catalytic soot oxidation

Catalysed soot oxidation is expected to decrease the soot oxidation temperature in a controlled fashion, thereby increasing efficiency and fuel economy.

Soot oxidation by O_2 occurs at a significant rate above 550 °C. The temperature inside the DPF is lower (200–450 °C) under normal driving conditions. Therefore catalysts that promote soot combustion at lower temperatures are required. But before reviewing different catalysts reported active for oxidation of diesel soot, it is also important to give some information about the mechanism of soot oxidation.

2.4.1 Mechanism of catalytic soot oxidation

Two different approaches can explain the catalytic oxidation of soot: "redox type oxidation" and "oxygen spillover".

The redox type oxidation mechanism, proposed by Amariglio and Duval [23], requires a physical contact between the catalyst and graphite (material used to understand soot oxidation mechanism) – direct contact.

Some catalysts can oxidise soot without having intimate physical contact – indirect contact. They catalyse the formation of a mobile compound (NO_2, O_{ads}, etc) that is more reactive than O_2. In the absence of physical contact, the formation of those mobile species is the main advantageous property of this type of catalyst. For indirect catalysts, two main reactions mechanisms are known: the NO_X aided gas-phase mechanism and the spill-over mechanism.

Cooper and Thoss [24] discovered a way of using gas-phase NO_2 as an activated mobile species for soot oxidation - NO_X aided gas-phase mechanism. They proposed that NO_2 accelerates soot combustion. In the spill-over mechanism (figure 4) catalysts can dissociate oxygen and transfer the activated oxygen atoms to the soot particle, where they it react as in a non-catalytic reaction.
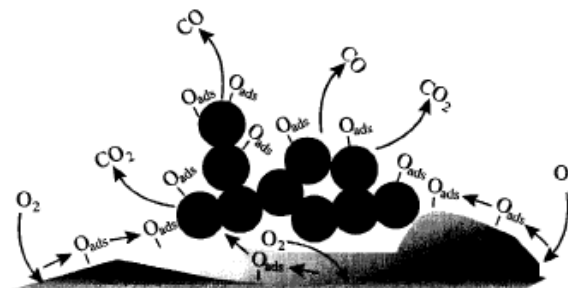
Figure 4 – Illustration of the spill-over mechanism on a catalyst surface. After [1]

It should be noted that most of the catalysts require a direct physical contact with soot. Therefore, for these catalysts, no matter how much they enhance soot oxidation, a good physical

contact should be provided. This was recognized by many scientists, and the studies have been focused on the catalysts having improved ability to enhance contact.

2.4.2 Catalysts for diesel soot oxidation

In the last two decades, a number of materials have been explored as catalysts for diesel soot oxidation. There are two kinds of catalysts: direct contact catalysts and indirect contact catalysts. The direct contact catalysts can oxidise soot only by intimate contact with soot, while in the indirect catalysts this is not necessary.

In spite of a lot of research on the subject, it is difficult to achieve direct contact between the catalyst and solid soot. Many catalysts were examined for their activity in diesel soot oxidation in the past years including oxides of Cu, Mo, Cr, Fe Pb and V [25]; Co/MgO, Co/K/MgO [26]; vanadates of Cs and K supported on alumina [27]; KCl promoted Cs and Cu vanadates [20], which were reported to oxidize soot in the temperature range of 350-450°C. These performances are, of course, strongly dependent on some parameters, such as the degree of contact between the soot and the catalyst, the model soot used, and the feed composition. As a result, it is difficult to compare the real performances without assessing the effects of each parameter. For that reason, some researchers adopted a certain terminology to compare the activities of the catalysts. For example, Neeft et al. [28] developed a definition about the degree of contact of soot with the catalyst, and some researchers used the same terminology thereafter. Two different contact modes were defined, depending on the way the powder catalyst and soot were mixed. They named "loose contact" when the catalyst powder is mixed with soot with a spatula and "tight contact" when a mechanical mill is used. Diesel soot filtered from the exhaust stream on a bed of catalysts particles is defined as "in-situ contact". For the same samples with different contacts a large difference in the combustion temperature (up to 200K) was found. The tight contact samples are more reactive because they have more points of contact with soot and the particles are smaller and more dispersed.

There are also mobile catalysts ($Cs_2SO_4 \cdot V_2O_5$, $CsVO_3 \cdot MoO_3$ and $KCl \cdot KVO_3$ [29-31]) that do not evaporate during soot oxidation - liquid catalysts. This type of liquid contact occurs both in laboratory test and pilot plant scale. Vanadates (V_2O_5) were the first catalysts that were considered to have extreme ability of contact to enhance, due to the high mobility of the surface metals inherent in their molten state nature [29-32].

The concept of molten catalysis then became popular and the studies were concentrated on the phase stabilization of these molten catalysts, since their vapour pressures were high for a possible exhaust application, causing the evaporation of the catalyst. Some phase stabilization techniques such as K doping of copper vanadates, were reported to enhance the stability [33].

A different way could be blending a stable organo-metallic additive into the fuel (10-100ppm) - fuel borne additives [34]. As a result, the catalyst–soot contact problem can be overcome, because the catalyst and the soot particles have more uniform dispersion. This leads to a higher intimate contact and decreases soot oxidation temperature by about 200 °C, compared with un-catalysed soot oxidation. The PSA Peugeot-system is an example of this type of catalyst [35].

NO_2 is a more powerful oxidant than O_2, and if enough NO_2 is present in the exhaust gas, soot can be oxidised around 350 °C. In catalysed soot filter (CSF) and continuously regenerating trap (CRT), NO in the exhaust gas is converted to NO_2 and NO_2 can oxidise the deposited soot in the filter. The above-mentioned after-treatment technologies (fuel borne additives and CRT) are already commercially available for decreasing particulate emissions from various sources. Cooper and Thoss [24] developed the NO_X-aided continuously regenerated trap (NO_X- aided CRT) for trucks and buses (passive regeneration). It consists of a wall-flow monolith with an upstream flow trough diesel oxidation catalyst, which is called, in this context, pre-oxidiser. The oxidation catalyst converts 90% of the CO and hydrocarbons present to CO_2, and 20-50% of the NO to NO_2. Downstream, the particles are trapped on a cordierite wall-flow monolith and, subsequently, oxidised by NO_2. The next table summarizes the catalysts and catalytic filter system for oxidation of diesel soot.

Table 3 - Classification of diesel soot oxidation catalysts [15].

Catalyst type/Chemical Process	Examples	Remarks
(1) Catalysis by mobile catalyst	Molten salt:	Based on C-O_2 reaction
	$Cs_2SO_4.V_2O_5$, $Cs_2O.V_2O_5$	Establish in-situ tight contact
	Ref:[29-31]	through soot wetting by the
	Volatile material:	catalyst
	Cu/K/V/Cl	Hydrothermal stability is low
	Ref:[25]	Discouraging investigations
(2) Fuel-borne catalysts	CeO_2, Pt-CeO_2	Based on both C-O_2 and C-NO_2
	Ref:[34]	reaction
	PSA-Peugeot system	Generates fine particle
	Ref:[35]	Requires DPF
(3) NO_X assisted soot oxidation	CRT-system	Based on the C-NO_2 reaction
	Ref:[24,22]	Uses Pt catalysts to generate NO_2
		Operates properly in lower
		sulphur level

Co_3O_4–CeO_2 [36] also showed excellent catalytic activity for soot oxidation, despite their low surface area. The promotional effects of an optimum amount of cobalt oxide incorporation in ceria and presence of a small amount of potassium appears to be responsible for the excellent soot oxidation activity of this mixed oxide type material. The catalytic materials show good thermal stability, while their low cost will also add to their potential for practical applications.

2.4.3 NO_X storage systems

In the last years a major part of the after-treatment research is focussed on NO_X conversion to N_2 over NO_X storage and reduction (NSR) catalysts or lean NO_X catalysts (LNC). The NO_X storage and reduction (NSR) catalysts store NO_X under lean conditions, typically as a nitrate at the average exhaust temperature, which is 200-250°C. Under rich conditions, the nitrate is readily reduced to N_2 leaving the catalyst ready to store NO_X again once lean conditions are re-established. One strategy for utilizing the NSR approach is to periodically operate the engine under both lean (i.e., excess oxygen) so-called *storage cycle* and rich (i.e., excess fuel) conditions so-called *reduction cycle*. The lean operation period should be much longer than the rich one in order to take advantage of the natural ''lean-burn'' condition of a diesel engine [13] [37].

NSR catalysts consist of a NO_X storage component (typically an alkaline or earth-alkaline metal oxide) and by a noble metal which reduces the stored NO_X. Early formulations developed by Toyota included Ba as NO_X storage compound and Pt as noble metal, but different formulations have also been patented [38] in order to optimize both the NO_X storage capacity and the NO_X reduction properties. Toyota Corporation developed the Pt/BaO/γ-Al_2O_3 [39]. In this catalyst formulation, the Pt component provides NO oxidation and NO_x reduction (redox) capabilities, whereas the primary role of BaO sites is NO_X storage in the form of $Ba(NO_3)_2$. The γ-Al_2O_3 support material enables dispersion of the active phases over a large surface area and may facilitate the reactant transport between the active sites on the catalyst via surface diffusion [39]. There are also NSR catalysts composed by Pt–Rh/Ba–Al_2O_3 and Pt–Rh/K–Al_2O_3 [40] and zeolite based catalysts [41]. Several catalysts like Pt/Al_2O_3, BaO/Al_2O_3, and Pt-BaO/Al_2O_3 were also investigated by Nova et al. to elucidate the NO_X storage mechanisms and the role of the noble metal in NO_X storage [42]. A general review of the NO_X storage and reduction technology is given by Epling [43].

The mains drawbacks of NSR system are the extreme need for high temperatures for the regeneration of the NO_X-trap and the sulphur sensitivity (this could be improved by reformulating the fuel) [17,18].

For the next legislations, both NO_X and soot levels have to be decreased to satisfactory levels, therefore SCR and soot oxidation catalytic systems have to be integrated. In order to make this kind of system Toyota has developed diesel particulate-NO_X reduction (DPNR) system, based on NSR catalysts, which can reduce NO_X to N_2 and simultaneously oxidise soot to CO_2 [40].

When the exhaust gas composition is abundant in O_2 (i.e., lean conditions), NO, which is the major NO_X component in the untreated exhaust gas mixture, is readily oxidized to NO_2 over Pt and NO_2 is stored as nitrates over the metal used via gas-phase adsorption and/or surface diffusion. Under rich conditions the stored nitrates are released in the form of NO_X, which is further reduced to N_2 by soot, resulting in regeneration of the active MeO (Me=metal) storage component. It is proposed that nitrates and active oxygen generated during storage and reduction steps are active soot oxidation species and, thereby, can decrease the oxidation temperature. NO_2 produced over noble metals of NSR catalysts can be trapped as nitrates and can also react with soot generating NO again. Under lean conditions the NSR system can be expected to function as CSF. It is also proposed that, under rich conditions active oxygen generated on the catalyst can oxidise the trapped soot [3].

A similar system is wanted for improving the soot oxidation in passenger cars. For that reason, NO_X assisted soot oxidation catalyst (active regeneration) has to be developed that later could be implemented in a catalytic filter. This catalyst will store NO_X at 200°C and release it at 450-550°C. Several catalysts have been reported, particularly Pt/Al_2O_3, $Pt/K–Al_2O_3$, $Pt/Ba–Al_2O_3$ [3] and also $Co,Ba,K/CeO_2$ [4]. However, only a part of the stored NO_X that is decomposed at high temperatures under lean conditions is found to be useful for soot oxidation. NO_X storage capacity decreases upon ageing under soot oxidising conditions. This will lead to a decreased soot oxidation activity on stored nitrate decomposition. $Pt/K–Al_2O_3$ catalyst is more active and more stable compared with $Pt/Ba–Al_2O_3$. The total NO_x storage capacity is similar over $Pt/K–Al_2O_3$ and $Pt/Ba–Al_2O_3$ and significantly higher than that of Pt/Al_2O_3 ($425 \mu mol/g_{cat}$) [3].

Also previous studies, using activated carbon supported metallic catalysts [44] [45], potassium bimetallic catalysts decrease effectively the temperature for the NO_X reduction. KCu and KCo showed some interesting results because, at low temperatures (300 °C), they combine a high capacity for NO_X reduction with a considerable consumption of carbonaceous material. Among the two bimetallic catalysts tested, KCo was the most active, achieving total NO_X reduction, to N_2, at 350 °C with the highest soot consumption rate [46].

In last year the catalysis group reported the NO_X assisted soot oxidation using Me/Al_2O_3- Pt, where Me is Ca, Ba, Mg, Sr was reported. Francesca Ricciardi has also study the influence of the surface area and the Sr concentration on NO_X storage and high temperature soot oxidation for %$Sr(NO_3)_2$ and %$Sr(NO_3)_2$+1%Pt/ZrO_2 [47-48].

2.4.4 NO_X assisted soot oxidation

Soot oxidation with oxygen can be used to regenerate the filter, however a significant reaction rate only occurs around 600°C, which very difficult to accomplish at normal operative conditions. Therefore, a more reactive compound with soot is necessary. NO_2 is a possible solution, since it is highly reactive with soot. In fact, NO_2 is able to oxidize soot at temperatures around 300°C. In figure 5, the reactivity of O_2 and NO_2 with soot is compared.
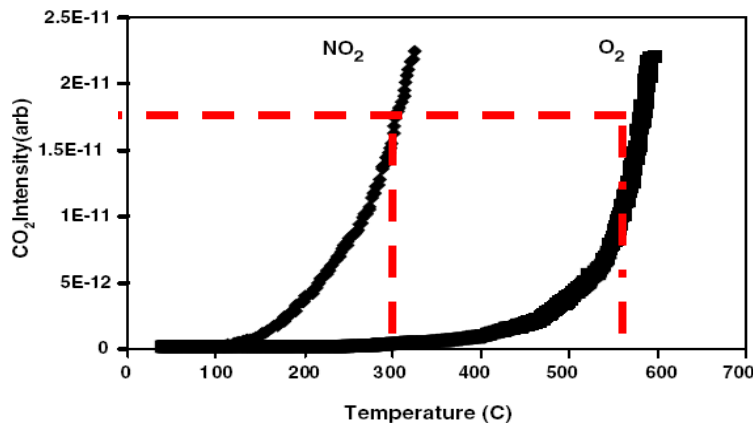
Figure 5 - Dependence of NO_2 and O_2 reactivity with soot from temperature [48].

However, NO_2 is present in diesel raw exhaust at very low concentrations (5-15% of total NO_X, or less than 50 ppm), which are not sufficient to provide the required reaction rates.

In order to increase the concentration of NO_2 in the exhaust gas it is necessary to put an oxidation catalyst in the upstream part of the filter. This catalyst (Pt) can oxidize NO to NO_2 with high efficiency. Therefore, the idea is to create a continuously regenerating trap concept, a system composed of a selective oxidation catalyst placed directly upstream of the particulate filter.

At temperatures of 300-350 °C, the oxidation catalyst starts to oxidize a portion of the NO in the exhaust stream to form NO_2, increasing the NO_2 fraction up to 50% of total NO_X [22].

Due to the stricter legislation, the interest in particulate filter regeneration systems using NO_2 for oxidizing soot (NO_2 assisted systems) has increased. This motivated some research works [5,6], nevertheless these works are few comparing with the importance of this issue.

In this work we studied the property of a storage material which will store the NO_X at temperatures below 300°C as nitrates and release it at the temperature of regeneration. If we add an oxidation catalyst the efficiency can be improved because the oxidation rate of soot and the recycling of NO to NO_2 is increased. It also increases the selectivities of complete oxidation reactions.

The NO_X storage-release cycle consists of two stages:

(1) Adsorption - The NO_X is "stored" from the gas flow by the catalyst at 200-250°C.

(2) Release - The NO_X is desorbed from the storage component at 500-600°C. This happens because most nitrates are decomposing at these temperatures.

This concept can be expressed in the following picture (using barium as example):
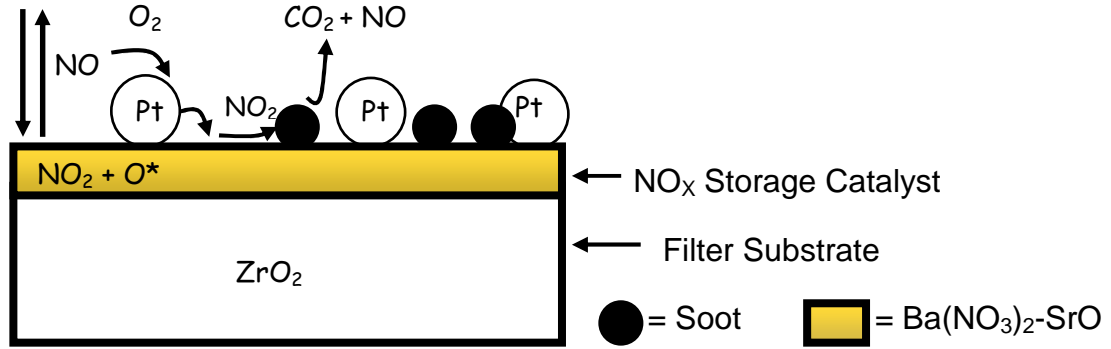
Figure 6 – NO_X storage-release

The basic principle of NO_X assisted soot oxidation can be explained by the following plan.

During storage conditions NO reacts with storage component (in the presented case it is barium nitrate) forming nitrites **(1)** and nitrates **(2)** in the catalyst:

$$BaO + 2NO + \frac{1}{2}O_2 \rightarrow Ba(NO_2)_2 \tag{1}$$

$$BaO + 2NO_2 + \frac{3}{2}O_2 \rightarrow Ba(NO_3)_2 \tag{2}$$
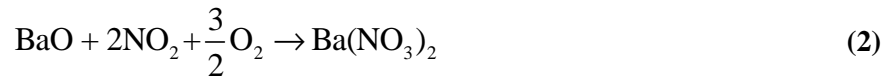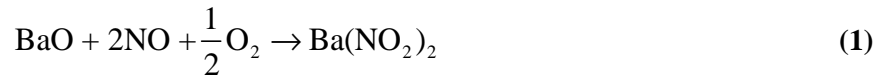
During the regeneration procedure the barium nitrate releases NO_X **(3)** by reverse reactions:

$$Ba(NO_3)_2 \rightarrow BaO + NO + NO_2 \tag{3}$$
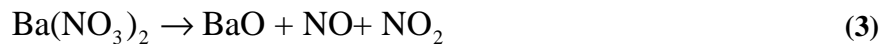
In the final step, an oxidation catalyst oxidizes NO into NO_2 **(4)** and then converts soot selectively into CO_2 and back to NO **(5)** which can participate in the next soot oxidation event:

$$2NO + O_2 \xrightleftharpoons{Pt} 2NO_2 \tag{4}$$

$$C + 2NO_2 \rightarrow CO_2 + NO \tag{5}$$

At higher temperatures the amount of NO_2 is smaller. As a result soot is mainly catalyzed by O_2 at temperatures above 600°C. Therefore, platinum is necessary to increase the efficiency of recycling NO to NO_2.

3. Objectives

Given the present state of research in NO_X assisted soot oxidation systems, given in the previous section, and the research done by Arkady Kustov and Francesca Ricciardi for the same research project, four objectives were set in the current study:

- To determine the influence of the catalyst composition on the NO_X storage/release and high temperature soot oxidation.

- Try to optimize catalyst composition in order to lower the temperature of soot oxidation.

- Compare the data for ZrO_2-supported systems with those previously obtained for Al_2O_3 previously by the Catalysis Engineering group.

- Optimize the efficiency of NO_X utilization for soot oxidation and find a catalyst with the best soot oxidation performance.

4. Experimental

This section focuses on the experimental work that was done to accomplish the goals for this project. The experimental work described is focused on the catalyst preparation and the equipments used for catalyst characterization.

4.1 Catalyst preparation

The first step in this work was the screening of the catalytic systems based on high-surface area ZrO_2 as support. This support was chosen because earth metals (alkaline and rare) and ZrO_2 are known to form nitrates upon reaction with NO_X. Also finally, platinum was introduced to increase oxidative function of the catalysts.

From previous research on the Catalysis group, was found that the best results were obtained for ZrO_2 with 90 m^2/g surface area. Furthermore, the best weight percentage for the catalyst supported was 20%. Therefore, a model NO_X storage system 20% $MeNO_3$ supported on ZrO_2 (90 m^2/g) where Me = Mg, Ca, Sr, Ba (alkaline earth metals) and La, Ce, Pr (rare-earth metals) was prepared.

The catalyst's support was prepared from pellets of ZrO_2 (provided by Alfa Aesar, a Johnson Matthey Company, 99% purity). The pellets of ZrO_2, were crushed in a mortar and sieved to obtain a fraction between 0.075 and 0.135 mm. Then the support was dried in the oven at 200°C for 2 hours, so that all water could be removed.

The supported catalysts were prepared by incipient wetness impregnation (IWI) of ZrO_2 support with an aqueous solution of corresponding salt, except for $Ba(NO_3)_2/ZrO_2$. Because of the low solubility of barium nitrate in water the liquid phase adsorption (LPA) technique was used. In typical catalyst preparation experiment 2 grams of ZrO_2 were impregnated with (2x0.8) ml/g of aqueous solution for the support. After impregnation the samples were dried for one hour at 120°C with a heating ramp of 5°C/min.

In the LPA technique 10ml of distilled water was added to a certain amount of barium nitrate (0.617g). This mixture was stirred and heated (60°C) for 2 hours so that all barium nitrates could be dissolved. The 2 g of the support then was added, stirred and heated during 4 hours (60°C). After adsorption the sample was filtered and then dried for 2 hours at 120°C with a heating ramp of 5°C/min.

To prepare platinum based catalysts, a platinum solution was prepared using $Pt(NH_3)_4Cl_2 \cdot H_2O$ (provided by Alfa Aesar, a Johnson Matthey Company, 56.4% purity) and then 1 gram of impregnated zirconia was impregnated with 0.8ml of Pt-containing solution. The sample then was dried for 2 hours at 120°C. This way, 1% of Pt was loaded in the catalyst. The concentrations of the metal nitrate and Pt solution used are in the following table:

Table 4 - Concentrations of $Me(NO_3)_2$ and $Pt(NH_3)_4 \cdot Cl_2$ in solution.

Sample	Final sample	$[Me(NO_3)_2]$, g/l	$[Pt(NH_3)_4 \cdot Cl_2]$,g/l
$Mg(NO_3)_2 \cdot 6 H_2O$	$20\% Mg(NO_3)_2/ZrO_2$	303	-
$Ca(NO_3)_2 \cdot 4 H_2O$	$20\% Ca(NO_3)_2/ZrO_2$	279	-
$Sr(NO_3)_2$	$20\% Sr(NO_3)_2/ZrO_2$	250	-
$Ba(NO_3)_2$	$20\% Ba(NO_3)_2/ZrO_2$	62	-
$La(NO_3)_2 \cdot 6 H_2O$	$20\% La(NO_3)_3/ZrO_2$	512	-
$Ce(NO_3)_2 \cdot 6 H_2O$	$20\% Ce(NO_3)_3/ZrO_2$	513	-
$Pr(NO_3)_2 \cdot 6 H_2O$	$20\% Pr(NO_3)_3/ZrO_2$	514	-
ZrO_2	$1\% Pt /ZrO_2$	-	18
$Ca(NO_3)_2 \cdot 4 H_2O$	$20\% Ca(NO_3)_2 + 1\% Pt /ZrO_2$	279	18
$Sr(NO_3)_2$	$20\% Sr(NO_3)_2 + 1\% Pt /ZrO_2$	250	18
$Ba(NO_3)_2$	$20\% Ba(NO_3)_2 + 1\% Pt /ZrO_2$	62	18
$La(NO_3)_2 \cdot 6 H_2O$	$20\% La(NO_3)_3 + 1\% Pt /ZrO_2$	512	18
$Ce(NO_3)_2 \cdot 6 H_2O$	$20\% Pr(NO_3)_3 + 1\% Pt /ZrO_2$	514	18

To conduct reproducible experiments and compare the various results thought out the years diesel soot with constant properties is required. Since the composition of diesel particles depends on many aspects, like motor characteristics (engine load, speed, life time) and way of collecting,

it is very difficult to find a suitable model. For that reason Degussa Printex U soot was chosen that shows properties in catalysed oxidation similar to "real soot". This industrial soot is produced by high-temperature pyrolysis. The next table shows the main properties of synthetic Printex U soot.

Table 5 – Chemical and Physical properties of Printex U synthetic soot [21].

Property	Value
Specific surface area	97 m^2/g
Ø primary particles	30nm
Hydrocarbons	5.2 wt%
C-content	92 wt%
H-content	0.6 wt%
N-content	0.2 wt%
S-content	0.4 wt%
Metal ash content	Below detection limit

4.2 Equipment

4.2.1 TGA

Thermogravimetric Analysis (TGA) is an analytical technique for measuring changes in mass as function of temperature. It is primarily used to determine the fraction of volatile components by monitoring the weight change that occurs as a specimen is heated. It is also used to analyze adsorption and desorption, reactions with purge gases, and ash content. From TGA curves, data on the kinetics and thermodynamics of the various chemical reactions, reaction mechanisms, reaction intermediates and final reaction products can be obtained. The measurement is normally carried out in air or in an inert atmosphere, such as helium or argon, and the weight is recorded as a function of increasing temperature.

The thermo gravimetric analysis (TGA) of the various samples was carried out in a Mettler Toledo, TGA/SDTA851^e instrument. The samples (around 30 mg) were placed in alumina crucibles and loaded into TGA sample tray.

Two different programs were used in TGA: *Air 900°C, 10°C/min* and *He 900°C, 10°C/min*. This means that the data presented in this study were obtained by heating up the sample from 25°C to 900°C in air with a constant rate of 10 °C/min. The same heating rate was also used with helium. Prior to sample analysis blank reference experiment with an empty crucible was always performed.

4.2.2 TPD-MS

TPD (temperature programmed desorption) involves heating a sample and simultaneously detecting the residual gas by means of a mass analyser – mass spectrometer (MS), that monitor the desorption products. As the temperature rises, certain absorbed species will have enough energy to escape and will be detected as a rise in pressure for a certain mass. The results of the experiment are the desorption rate of each product species versus the temperature.

In modern implementations of the technique the detector of choice is a small, quadrupole mass spectrometer (QMS) and the whole process is carried out under computer control with quasi-simultaneous monitoring of a large number of possible products.

During this work the temperature programmed desorption-decomposition (TPD) was carried out in a tubular quartz reactor (5mm internal diameter) located in the high temperature furnace using MS analysis of the products. In the typical experiment approximately 200 mg of sample (previously diluted with SiC to a ratio of 1:6) was packed between two quartz wool plugs and heated from room temperature to 900°C with a heating rate of 5°C/min, in a flow of 10 ml/min of O_2 and 40 ml/min of He.

Decomposition of bulk nitrates, soot oxidation and storage-release cycles were performed using this equipment. Below it will be explained how soot oxidation and storage-release were performed.

Soot Oxidation

To perform soot oxidation, soot was mixed with the catalyst and diluted with SiC in a 1:20:120 weight proportion. The TPD is a good method to see how bulk and surface nitrates are decomposed and also to determine the conversion of soot. By this method it is possible to monitor the signal of each compound, which is proportional to the concentration of the product desorbing from the sample. The nitrates start to decompose with the increase of temperature, releasing nitrogen dioxide, which reacts with the soot forming carbon monoxide and carbon dioxide and back to nitrogen monoxide. The mass spectrometer permits the continuous monitoring of the formed products.

The soot conversion and selectivity of soot oxidation to CO_2 can be quantified as function of temperature and assuming complete soot oxidation at the end of the experiment at 900°C. The soot conversion can be calculated by the following equation:

$$\text{Conversion (\%)} = \frac{S_{CO}(T) + S_{CO_2}(T)}{S_{CO}^{tot} + S_{CO_2}^{tot}} \times 100 \qquad \textbf{(6)}$$

where, $S_{CO}(T)$ and $S_{CO2}(T)$ represent the areas under the CO and CO_2 curves at a certain temperature, respectively. It is also assumed that all soot is converted to CO and CO_2 at the end of the experiment.

The selectivity to CO_2 can be calculated dividing the total area under the CO_2 curve to the sum of the areas under the CO and CO_2 curve, as is represented in the following equation:

$$\text{Selectivity (\%)} = \frac{S_{CO_2}^{tot}}{S_{CO}^{tot} + S_{CO_2}^{tot}} \times 100 \tag{7}$$

This temperature control in TPD-MS equipment is not very precise comparing with the TGA. The temperature difference between two techniques for similar experiments (like bulk nitrates decomposition) can reach almost 100°C. This means that bulk nitrates decompose at ~100°C lower temperature in TGA. This happens mainly because the detector in TPD takes longer time to detect the signal of each compound and also the furnace is not excellent.

Storage-Release cycles

The storage release cycles for all the samples were also studied in TPD-MS. In this case a bottle containing 2.5% NO_2 in He was added, which makes it possible to do the adsorption step. The storage release cycles are divided in three steps: bulk nitrate decomposition, adsorption of NO_X and desorption of nitrates, which are described in more details further.

1. Bulk Nitrate Decomposition – In this step approximately 200 mg of sample (previously diluted with SiC to a ratio of 1:6) was packed between two quartz wool plugs and heated from room temperature to 700°C with a heating rate of 10°C/min, in a flow of 10 ml/min of O_2 and 40 ml/min of He. With the increase of temperature the nitrates start to decompose (NO signal increase) from the sample according to the following reaction (as an example it is presented for the barium nitrate):

$$\text{Ba(NO}_3)_2/\text{ZrO}_2 \rightarrow Ba\text{O/ZrO}_2 + 2\text{NO} + \frac{3}{2}\text{O}_2 \tag{8}$$
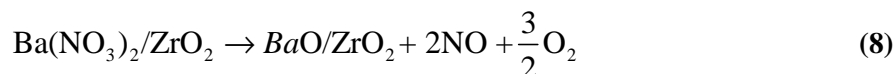
Using the area under the NO curve it is possible to define the maximum possible NO_X storage capacity, since the amount of storage component is known.

2. Adsorption of NO_X at 200°C – The second step was the adsorption of NO_X. The He and O_2 flow were switched off and a bottle of 2.5% of NO_2 in He was opened with a flow of 10

ml/min. The sample was treated with this mixture at 200°C for 30 minutes. During adsorption step nitrates are formed on the surface of the catalyst according to the following reaction:

$$BaO/ZrO_2 + 3NO_2 \rightarrow Ba(NO_3)_2/ZrO_2 + NO \tag{9}$$
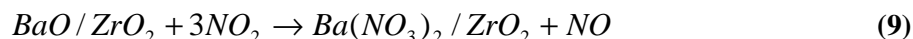
3. Desorption of nitrates – In the third step, the flow of 2.5% NO_2 in He was switched off and the O_2 and He flows were switch on. Desorption of the surface nitrates happened following the same conditions as in the decomposition step. The desorbed species were again detected by MS. From the area under desorption curve it was possible to calculate the actual NO_X storage capacity of the system according to the following equation:

$$NO_X \text{ Storage Capacity} = \frac{NO_X \text{stored}}{\text{maximum possible } NO_X} \times 100\% \tag{10}$$

4.2.3 Diesel Six-Flow Reactor

For study of the soot oxidation with different operative modes the diesel six-flow reactor was used (Fig. 9). This equipment is very similar to TPD, but instead of only one reactor, it is possible to operate with six reactors at the same time, using the same operative conditions.

The diesel six-flow reactor can be divided in three sections: gas mixing, reactor, analysis.

The gas-mixing is where the inlet gas that goes for the reactors can be mixed with plenty of compounds, such as Ar, O_2, NO, NO_2, CO, propene and SO_2. The flow of each compound and total flow are controlled by mass flow controllers (Brooks 5850 E).

In the reactor section six quartz-glass reactors with an outer diameter of 10 mm and an inner diameter of 7 mm were placed in an oven. Each sample (containing SiC+soot+catalyst) was mixed and packed between two quartz wool plugs. The gas mixture from the mixing section gas then passed through a heated glass bed and then was led through each reactor (in down flow) using mass flow controllers. The pressure upstream of each reactor was measured with a Kulite ITQ-1000-100-A pressure transducer. The oven temperature was controlled with an Eurotherm 818P programmable controller. The temperature in each reactor was measured with Nicrosil thermocouples positioned on top of the soot bed. The entire reaction section, including the mass flow controllers, was placed in a heated cabinet at 75°C. The outlet gas of the reactor was guided through a Valco 6-way selection valve that leads the outlet gas of one of the reactor to the analysis section and that of the other reactors to the vent. The composition of each reactor outlet was analysed every 12 minutes (2 minutes/reactor).

To study the behaviour of the catalyst in different operative conditions, four sets of experiments were made. The experimental conditions are described in Appendix C.

4.2.4 FTIR-MS

In infrared spectroscopy, IR radiation is passed through a sample. Some of the infrared radiation is absorbed by the sample and some of it is passed through (transmitted). The resulting spectrum represents the molecular absorption and transmission, creating a fingerprint of the sample. Like a fingerprint no two unique molecular structures produce the same infrared spectrum. The different catalysts were analyzed by FTIR-MS (Fourier Transform Infrared associated with a mass spectrometer). Experiments were preformed in a Thermo Nicolet Nexus spectrometer using Spectratech diffuse reflectance accessory equipped with a high temperature cell – drift cell. The sample (around 50 mg) was placed into the high-temperature quartz cell. The NO_X storage-release cycles were studied by similar manner as TPD-MS, but with FTIR-MS it was also possible to collect and process the spectra from the samples using the OMNIC$^{®}$ software. The same steps were used in the FTIR and in TPD-MS, only with minor variances in the conditions. During the first phase the temperature was increased from 200°C to 600°C at a 100°C steps (heating rate of 1800°C/h) followed by an isotherm of 20 min at each temperature. As was mentioned before, the nitrates start to decompose by increasing the temperature, releasing NO. After decomposition of bulk nitrates the background spectrum was collected on going back from 600°C to 200°C with 100°C steps.

In the second step – adsorption – the sample was treated with a flow of 800ppm of NO + 20% of O_2 at 200°C during 3 hours. The molecules of NO were adsorbed on the surface of the catalyst over the time. The spectrum was collected for 1, 3, 5, 10, 15, 20, 30, 45, 60, 90, 120, 150 and 180 minutes after the start of adsorption.

The last phase - desorption of nitrates - was completed is the same conditions as the first (decomposition of bulk nitrates). During the desorption of stored nitrates spectra were collected from 200°C to 600°C with 100°C steps. From the area under the desorption curve, it was possible to calculate the actual NO_X storage capacity of the system.

5. Results

5.1 TGA

Thermogravimetric analysis (TGA) gives us information about the temperature of the decomposition of the nitrates. Standard TGA output is the weight loss in the samples as a function of time or temperature. Figure 7 shows a typical TGA pattern, comparing the air programme and helium programme for $Ba(NO_3)_2/ZrO_2$.
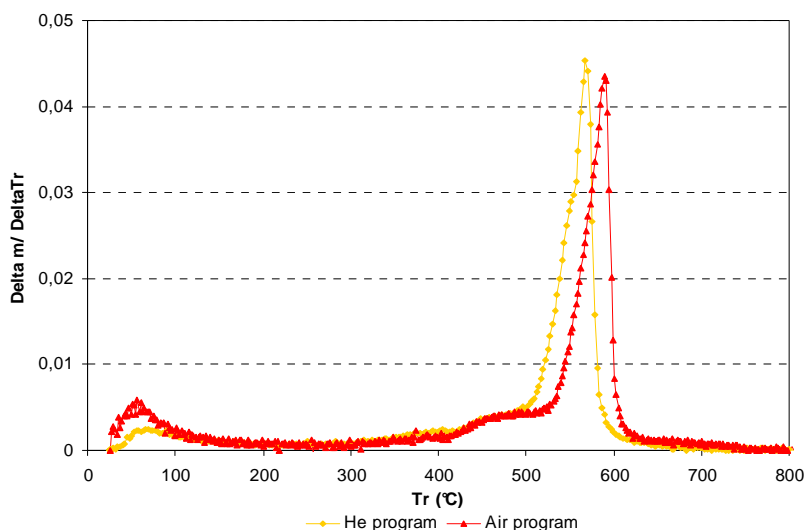
Figure 7 - TGA analysis of $Ba(NO_3)_2/ZrO_2$ using Air program and He program.

Different programs (air and helium) were used to see if the composition of the gas influences the decomposition of nitrates. In both programs temperature is increased from room temperature to 900°C, although different gas composition is used. Comparing the results obtained for the different programs it is possible to see that nitrates decomposition in air happens at somewhat higher temperatures. This happens because the decomposition of nitrates (for example barium nitrate), is reversible (reaction 11).

$$Ba(NO_3)_2 \leftrightarrow BaO + 2NO + O_2 \tag{11}$$
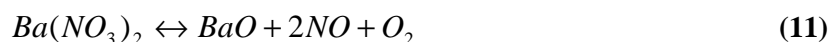
In the case of decomposition in air, the concentration of O_2 increases and the reaction shifts towards barium nitrate. So, in the air program higher temperatures will be necessary to decompose the nitrates. For the sake of brevity, all the other TGA data are presented in appendix A. In Figures 8 and 9 different systems measured using the air program are compared.
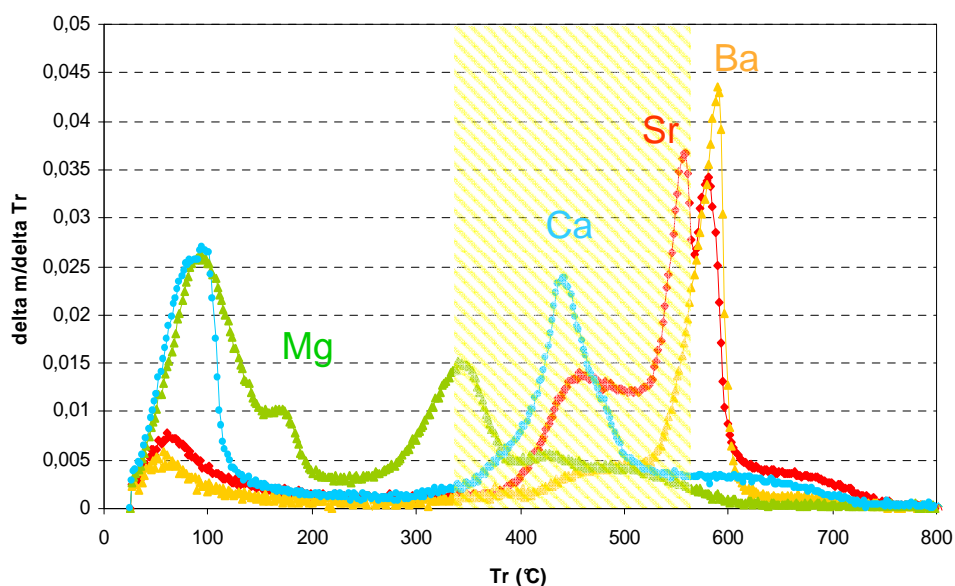
Figure 8 - TGA profiles of Mg, Ca, Sr and Ba- based system using the air program.
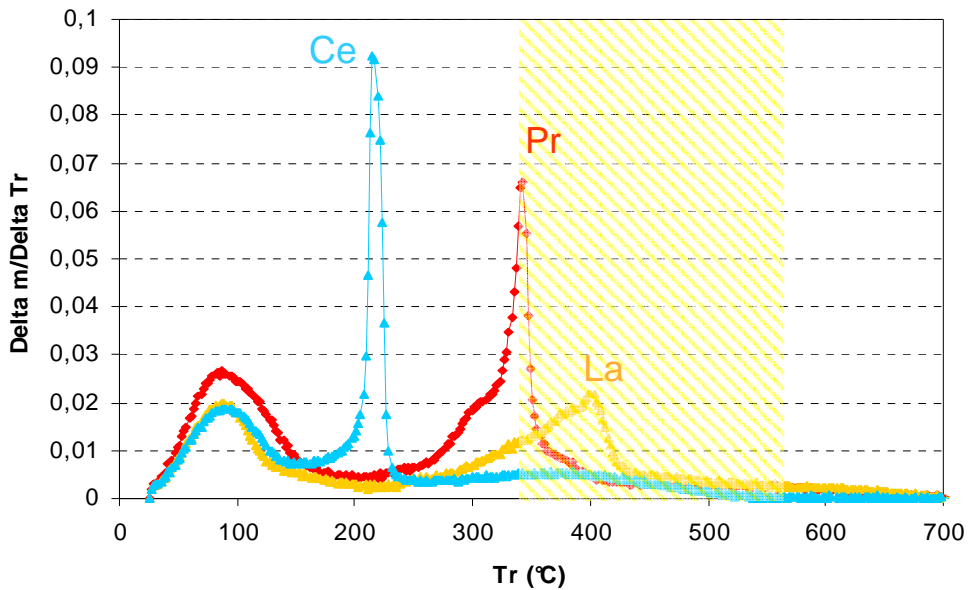
Figure 9 - TGA profiles of Ce, La and Pr- based system using the air program.

For the practical application in soot trap as mentioned previously, storage compound should release nitrates at temperatures above 400°C. According to results shown on figures 8 and 9, Sr, Ca, La and Pr-based systems look more promising because in their case nitrates are mainly decomposed between 350 and 550°C. Cerium and magnesium nitrates decompose too early. But this is just bulk nitrates and we are of course more interested in actual stored nitrates therefore the next step is to study all these systems in the storage-release cycles. In table 6 and 7 temperatures of nitrates decomposition and theoretical and practical weight losses (before and after 200°C) are compared for the air and helium programs.

Table 6 – Practical and Theoretical Weight Loss of the samples using the Air program.

Sample	T max, °C				Weight Loss, %		Theoretical Weight Loss, %
	T1	T2	T3	T4	<200°C	>200°C	
ZrO_2	65	-	-	-	2.8	1.5	-
$Mg(NO_3)_2$-ZrO_2	93	171	343	427	9.5	8.8	20.4
$Ca(NO_3)_2$-ZrO_2	99	443	-	-	6.6	9.8	17.0
$Sr(NO_3)_2$-ZrO_2	65	457	559	581	1.9	12.0	10.2
$Ba(NO_3)_2$-ZrO_2	61	591	-	-	1.7	10.5	10.2
$La(NO_3)_3$-ZrO_2	95	403	-	-	7.0	12.7	25.5
$Ce(NO_3)_3$-ZrO_2	95	215	390	-	7.4	9.6	25.5
$Pr(NO_3)_3$-ZrO_2	91	343	-	-	7.3	12.8	25.5

Table 7 – Practical and Theoretical Weight Loss of the samples using the He program.

Sample	T max, °C				Weight Loss, %		Theoretical Weight Loss, %
	T1	T2	T3	T4	<200°C	>200°C	
ZrO_2	71	-	-	-	2.7	1.3	-
$Mg(NO_3)_2$-ZrO_2	87	151	338	428	9.1	8.4	20.4
$Ca(NO_3)_2$-ZrO_2	77	437	-	-	6.1	9.7	17.0
$Sr(NO_3)_2$-ZrO_2	81	455	543	-	2.0	10.4	10.2
$Ba(NO_3)_2$-ZrO_2	63	567	-	-	1.8	11.4	10.2
$La(NO_3)_3$-ZrO_2	80	394	506	-	7.5	12.5	25.5
$Ce(NO_3)_3$-ZrO_2	85	213	379	-	8.1	9.3	25.5
$Pr(NO_3)_3$-ZrO_2	85	338	-	-	7.0	12.0	25.5

The weight loss before 200°C in the samples is about 2%, namely because of the water, except in the case of Mg $(NO_3)_2$/ZrO_2, $Ce(NO_3)_3$/ZrO_2, $La(NO_3)_3$/ZrO_2, and $Pr(NO_3)_3$/ZrO_2. Their weight loss before 200°C is much larger because samples used also have incorporated water [$Mg(NO_3)_2 \cdot 6\ H_2O$; $Ce(NO_3)_3 \cdot 6\ H_2O$; $La(NO_3)_3 \cdot 6\ H_2O$; $Pr(NO_3)_3 \cdot 6\ H_2O$] and also in the case of Mg $(NO_3)_2$/ZrO_2 and $Ce(NO_3)_3$/ZrO_2 the decomposition of nitrates start before 200°C. In $Ca(NO_3)_2$/ZrO_2 the weight loss is relatively smaller because the sample used only had 4 molecules of water ($Ca(NO_3)_2 \cdot 4\ H_2O$). In principle all the samples should have theoretical weight loss of 10.2%, like $Sr(NO_3)_2$/ZrO_2 and $Ba(NO_3)_2$/ZrO_2. In the of Mg $(NO_3)_2$/ZrO_2 and $Ca(NO_3)_2$/ZrO_2 weight loss is higher because of the water incorporated and for the rare-earth metals one extra NO_3 anion accounts for higher weight losses.

5.2 TPD-MS

Temperature programmed desorption-decomposition (TPD) was used to study soot oxidation and storage release cycles. In soot oxidation the temperature was increased from 25°C until 900°C. During increasing of the temperature nitrates start to decompose and release NO_2, which reacts with soot forming CO, CO_2 and back NO. In the following figure a typical TPD profile is shown (La based-system). All the other curves are given in Appendix B1. In the case of the TPD-MS set up a 0.5:1 N/C ratio was used

The results for soot oxidation for all samples are summarized in the table 8.
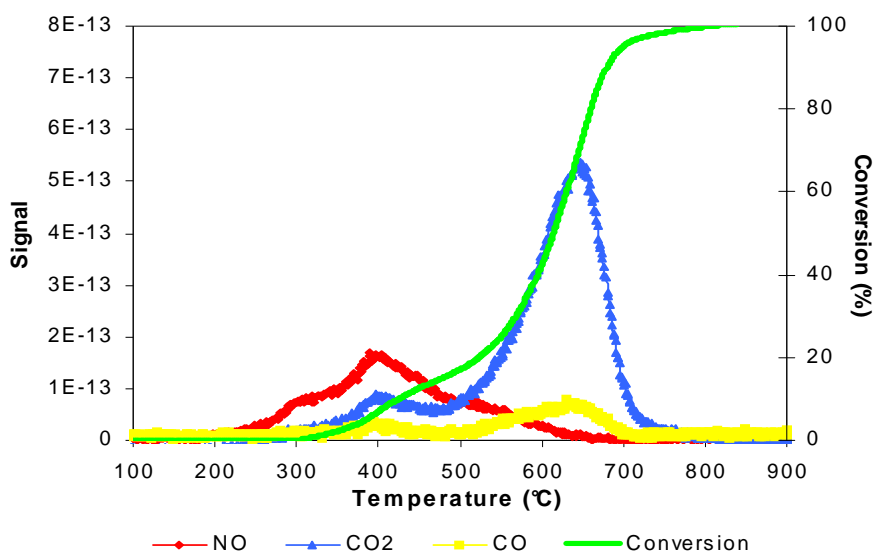
Figure 10 - TPD profiles of CO_2, CO and NO signals and calculated soot conversion for 20%La(NO$_3$)$_3$/ZrO$_2$ mixture with soot.

Table 8 – Temperature of the max peak of CO_2, 20% and 50% conversion of soot, nitrate decomposition and soot conversion at 500°C and the selectivity obtained.

Sample	$T_{max\ peak}$ (°C)	$T_{20\%\ conv}$ (°C)	$T_{50\%\ conv}$ (°C)	$T_{nitrate\ peak}$ (°C)	$Conv_{500°C}$ (%)	Selectivity (%)
Soot+ZrO$_2$	650	580	634	-	6.8	79.6
Soot+20%Mg(NO$_3$)$_2$ / ZrO$_2$	660	524	590	370	15.9	83.3
Soot+20%Ca(NO$_3$)$_2$ / ZrO$_2$	630	516	603	476	16.0	83.1
Soot+20%Sr(NO$_3$)$_2$ / ZrO$_2$	600	530	605	560	12.8	82.9
Soot+20%Ba(NO$_3$)$_2$ / ZrO$_2$	650	550	616	663	9.6	82,6
Soot+20%La(NO$_3$)$_3$ / ZrO$_2$	650	512	613	404	17.2	84.3
Soot+20%Ce(NO$_3$)$_3$ / ZrO$_2$	653	570	629	260	6.7	89.9
Soot+20%Pr(NO$_3$)$_3$ / ZrO$_2$	645	506	604	370	18.7	81.8

In Table 8 temperatures of maximum peak of CO_2 and of 20% and 50% soot conversion as well as amount of soot converted up to 500°C are given to provide the comparison between different systems. Selectivities of soot conversion to CO_2 are also shown. The $T_{nitrate\ peak}$ is also shown which corresponds to the temperature at which the highest NO signal during the decomposition of the nitrates is obtained. Analysing table 8 it is easy to observe that Ca, Sr, La and Pr-based systems show lower soot oxidation temperatures and therefore look more promising for further investigations. In Mg and Ce based-systems the nitrates decompose at lower temperatures; as a result the NO_X is not used so efficiently for oxidizing soot. TGA and TPD-MS data show similarities in the curves of decomposition of nitrates (NO signal). Finally Pt was added to increase the oxidation rate. The results obtained are shown in the table 9.

Table 9 – Temperature of the max peak of CO_2, 20% and 50% conversion of soot, nitrate decomposition peak and soot conversion at 500°C and the selectivity obtained for Pt-containing catalysts.

Sample	$T_{max\ peak}$ (°C)	$T_{20\%\ conv}$ (°C)	$T_{50\%\ conv}$ (°C)	$T_{nitrate\ peak}$ (°C)	$Conv_{500°C}$ (%)	Selectivity (%)
Soot+1%Pt-ZrO$_2$	642	581	627	-	4.2	93.4
Soot+20%Ca(NO$_3$)$_2$ +1%Pt-ZrO$_2$	650	505	597	440	19.2	88.4
Soot+20%Sr(NO$_3$)$_2$ +1%Pt-ZrO$_2$	623	487	581	480	24.1	91.9
Soot+20%Ba(NO$_3$)$_2$ +1%Pt-ZrO$_2$	605	536	586	650	8.6	93.2
Soot+20%La(NO$_3$)$_3$ +1%Pt-ZrO$_2$	572	483	580	312	22.8	86.8
Soot+20%Pr(NO$_3$)$_3$ +1%Pt-ZrO$_2$	644	502	579	305	19.7	93.4

The presence of platinum on the surface of the catalyst influences soot oxidation since Pt increase the oxidation rate, and the recycling of NO to NO_2. Therefore after adding platinum, all the samples achieved higher conversions at the same temperature and of course higher selectivities to CO_2. Sr based system showed highest conversions at 500°C (24.1%), while La had the lowest temperature of 20% of conversion (483°C).

The TPD was also used to study the storage-release cycles of the different samples. With this equipment it is possible at the same time to see what happens on the surface of the catalyst and detect what products are coming out of the system. The TPD-MS was used according to the following steps: decomposition of bulk nitrates, adsorption of NO_X and desorption of nitrates. They are explained in detail in the Experimental section.

In figure 11 the NO decomposition and the NO desorption curves are compared (Ca based-system). Dividing the area under the curve of desorption for the area under the curve of decomposition it is possible to calculate the storage capacity. For the sake of brevity all the curves for decomposition and desorption of the samples are presented in Appendix B2.
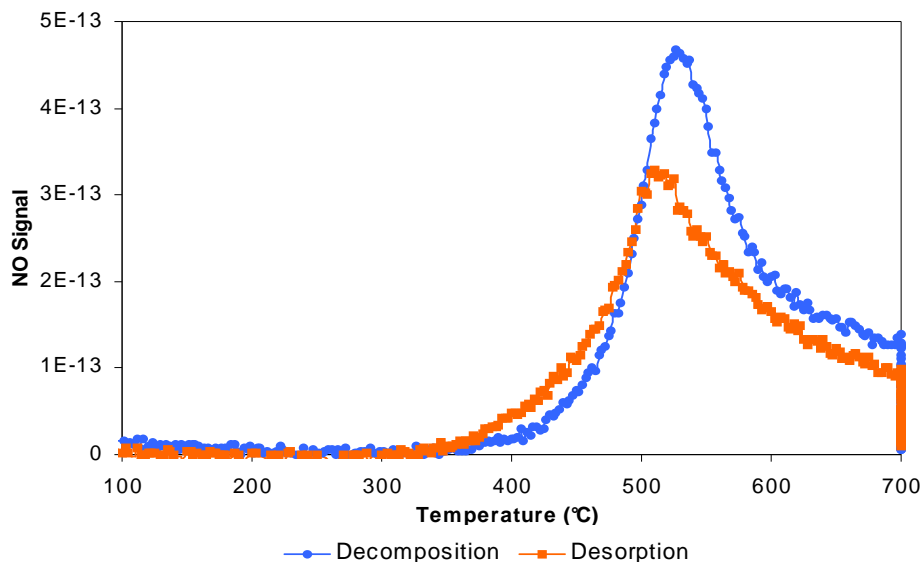
Figure 11 - Decomposition and desorption of nitrates for $20\%Ca(NO_3)_2$ /ZrO_2 sample (in a flow of 50 ml/min of air) with increasing of temperature from 25°C to 700°C at a heating rate of 10°C/min followed by an isotherm of 20 min at 700°C.

The storage-release cycles were performed for most of the studied systems and the results are summarized in Table 10. The absolute NO_X storage capacity is proportional to the amount of bulk nitrates introduced. Since they have different molar weight the absolute bulk nitrates in each sample will be different.

Table 10 – NO_X Storage Capacities of different samples obtained from TPD-MS results.

Sample	$T_{Dec/Des}$ (°C)	Relative NO_X Storage Capacity (%)	Measured NO_X Storage Capacity (μmol/g)	Absolute NO_X Storage Capacity (μmol/g)	NO_X released between 200°C and 500°C (%)
ZrO_2	-/340	-	-	36.1	45.3
20% $Mg(NO_3)_2$-ZrO_2	296/343	47.6	450	945.1	41.2
20% $Ca(NO_3)_2$-ZrO_2	444/422	91.0	860	944.3	35.5
20% $Sr(NO_3)_2$-ZrO_2	493/427	61.1	577	945.0	25.3
20% $Ba(NO_3)_2$-ZrO_2	534/433	39.7	375	943.8	19.6
20% $La(NO_3)_3$-ZrO_2	325/382	45.3	570	1258.4	48.2
20% $Ce(NO_3)_3$-ZrO_2	229/329	24.2	304	1256.7	72.4
20% $Pr(NO_3)_3$-ZrO_2	332/328	37.1	467	1256.8	60.8
20% $Sr(NO_3)_2$+1%Pt-ZrO_2	308/363	63.7	602	945.0	52.8
20% $La(NO_3)_3$+1%Pt-ZrO_2	305/300	43.6	548	1258.4	63.1
20% $Pr(NO_3)_3$+1%Pt-ZrO_2	285/258	36.9	464	1256.8	67.8

Ca and Sr based-system are the most promising systems since they can store more nitrates. Also the incorporation of Pt on the surface of the catalyst does not have much influence on storage capacity, nevertheless the percentage of NO_X released between 200°C and 500°C increases. This observation will be further discussed in more detail in section 6.

5.3 Diesel Six-flow Reactor

Diesel six-flow reactor was used to study soot oxidation for different samples at different operative condition. To evaluate the effect of different operative modes on the soot oxidation, the experiments were done in four different conditions. The different operative modes are described in the Experimental section. All parameters were calculated for all analyzed sample, by the same way as in the TPD. The results are summarized in the next tables. The soot oxidation graphs of the samples are in Appendix C.

Table 11 – Results for soot oxidation on six-flow reactor set-up (first experiment).

Reactor	Sample	$T_{max\ pic}$ (°C)	$T_{20\%conv}$ (°C)	$T_{50\%conv}$ (°C)	$Conv_{500°C}$ (%)	Selectivity (%)
1	Soot+20%Sr(NO$_3$)$_2$ / ZrO$_2$	506	426	485	63.5	94.7
2	Soot+20%Pr(NO$_3$)$_3$ / ZrO$_2$	504	428	482	65.5	93.2
4	Soot+20%La(NO$_3$)$_3$ / ZrO$_2$	506	419	482	66.4	80.4
5	Soot+20%Ba(NO$_3$)$_2$ / ZrO$_2$	500	424	478	68.8	81.8

These results appear to be better than those obtained by TPD, because higher conversion of soot is obtained at lower temperatures. However, it is hard to see any difference between the 4 samples (error within ±3°C). The possible solution is to use higher catalyst/soot ratios. It is well-known that the set up cannot be directly compared with the TPD-MS since the catalyst-soot ratio and also the heating rates are different. With a slow heating rate it is more difficult to take advantage of the NO$_X$ assisted soot oxidation. In the second experiment (table 12) platinum was added to increase the oxidation rate, and therefore increase the recycling of CO to CO$_2$. In table 13 the uncatalysed system (with and without Pt) and the Ca-based systems are compared. The difference between the third and forth experiment is that in the last case the samples used were calcined at 500°C during 5 hours (table 14). In the fourth experiment there was an isotherm at 200°C where the samples could store NO$_X$ as nitrates.

Table 12 - Results for soot oxidation on six-flow reactor set-up (second experiment).

Reactor	Sample	$T_{max\ pic}$ (°C)	$T_{20\%conv}$ (°C)	$T_{50\%conv}$ (°C)	$Conv_{500°C}$ (%)	Selectivity (%)
1	Soot+1%Pt+20%Sr(NO$_3$)$_2$ / ZrO$_2$	507	419	485	66.4	97.2
2	Soot+1%Pt+20%Pr(NO$_3$)$_3$ / ZrO$_2$	498	424	480	69.6	96.8
4	Soot+1%Pt+20%La(NO$_3$)$_3$ / ZrO$_2$	498	425	480	69.8	97.4
5	Soot+1%Pt+20%Ba(NO$_3$)$_2$ / ZrO$_2$	500	423	480	70.8	97.3

Table 13 - Results for soot oxidation on six-flow reactor set-up (third experiment).

Reactor	Sample	$T_{max\ pic}$ (°C)	$T_{20\%conv}$ (°C)	$T_{50\%conv}$ (°C)	$Conv_{500°C}$ (%)	Selectivity (%)
1	Soot+20%Ca(NO$_3$)$_2$ / ZrO$_2$	513	427	491	59,0	86,9
2	Soot+1%Pt+20%Ca(NO$_3$)$_2$ / ZrO$_2$	509	428	486	64,1	97,4
4	Soot+ ZrO$_2$	507	432	488	62,7	85,8
5	Soot+1%Pt / ZrO$_2$	500	428	485	65,1	96,8

Table 14 - Results for soot oxidation on six-flow reactor set-up (fourth experiment).

Reactor	Sample	$T_{max\ pic}$ (°C)	$T_{20\%conv}$ (°C)	$T_{50\%conv}$ (°C)	$Conv_{500°C}$ (%)	Selectivity (%)
1	Soot+20%CaO / ZrO$_2$	509	439	492	58,3	86,1
2	Soot+1%Pt+20%CaO / ZrO$_2$	506	438	486	63,4	98,1
4	Soot+ ZrO$_2$	507	439	488	62,4	87,1
5	Soot+1%Pt / ZrO$_2$	509	438	489	61,3	97,8

Comparing the catalyst-soot ratios used in the two equipments, it is possible to notice that in diesel six-flow the N/C ratio is only around 0.1:1 versus 0.5:1 in TPD experiments, for that reason the effect of nitrates is not as prominent as in the case of TPD experiments. All the experiments do not show big differences between the various systems. Comparing the rare earth metals with the alkali-earth metals that have smaller amounts of nitrates, the results are the same. This can be explained by the low ratio of nitrates that was used in the experiments.

Although similar trends were not found we can say that when platinum is added the selectivity to CO_2 and the conversion of soot are increased.

It would be expected in the forth experiment (samples calcined) to obtain lower conversions at 500°C, however the conversions are similar to the third experiment, indicating again the fact that it is necessary to increase the catalyst:soot ratio.

5.4 FTIR-MS

The FTIR-MS was performed for four catalysts: ZrO_2, $20\%Ca(NO_3)_2/ZrO_2$ $20\%Sr(NO_3)_2/ZrO_2$ and $20\%La(NO_3)_3/ZrO_2$ using the drift cell. By this method it was possible to record at the same time the mass signal of each compound released, and the spectra of each sample. This study was performed in three phases:

In the first phase - ***decomposition of the bulk nitrates*** - temperature was increased from 200°C to 600°C leading to the decomposition of the bulk nitrates as can be seen in the graph below. Figure 12 shows the bulk nitrates decomposition for the $20\%Ca(NO_3)_2/ZrO_2$ sample. The other curves are not presented for sake of brevity but are reported in the Appendix D1 and show similar trends.
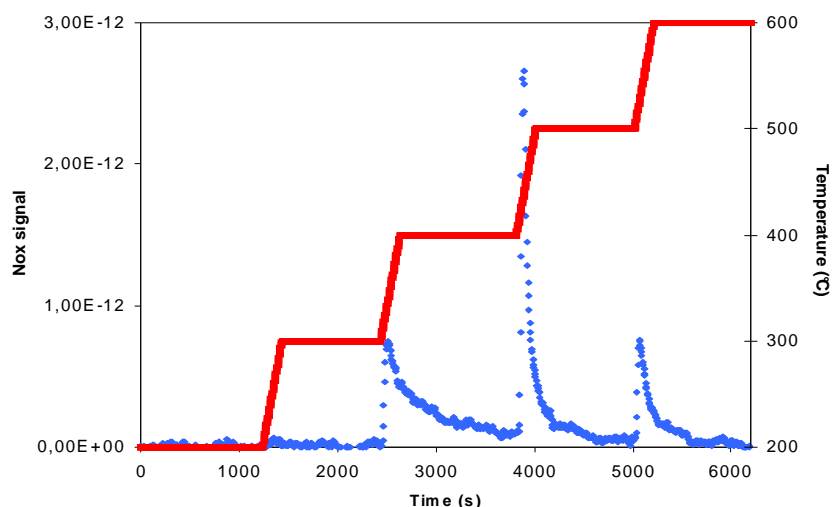

Figure 12 - Decomposition of bulk nitrates for $20\%Ca(NO_3)_2$ /ZrO_2 sample (in a flow of 30 ml/min of air) with increasing of temperature from 200°C to 600°C with a 100°C steps, heating rate of 1800°C/h followed by an isotherm of 20 min at each temperature (red-T;blue-NO_X signal).

The maximum of bulk nitrate decomposition is observed, for the all the samples, between 400°C and 500°C. Using the area under the decomposition curve it is possible to know how much nitrates are stored in the beginning assuming that all nitrates are decomposed at the end. In the end of bulk nitrate decomposition the background spectra was collected from 600°C to 200°C.

After decomposition of bulk nitrates ***adsorption of NO$_X$ at 200°C*** was performed. The samples were treated with 800 ppm of NO +20% O$_2$ in He during 3 hours. Over the time, the nitrates start to form in the surface of the catalyst and the spectrum was recorded during 180 minutes to ensure that steady-state was achieved. The spectra corresponding to NO adsorption for ZrO$_2$ and 20%Ca(NO$_3$)$_2$/ZrO$_2$ are shown in Figure 13(a and b):

a)

b)
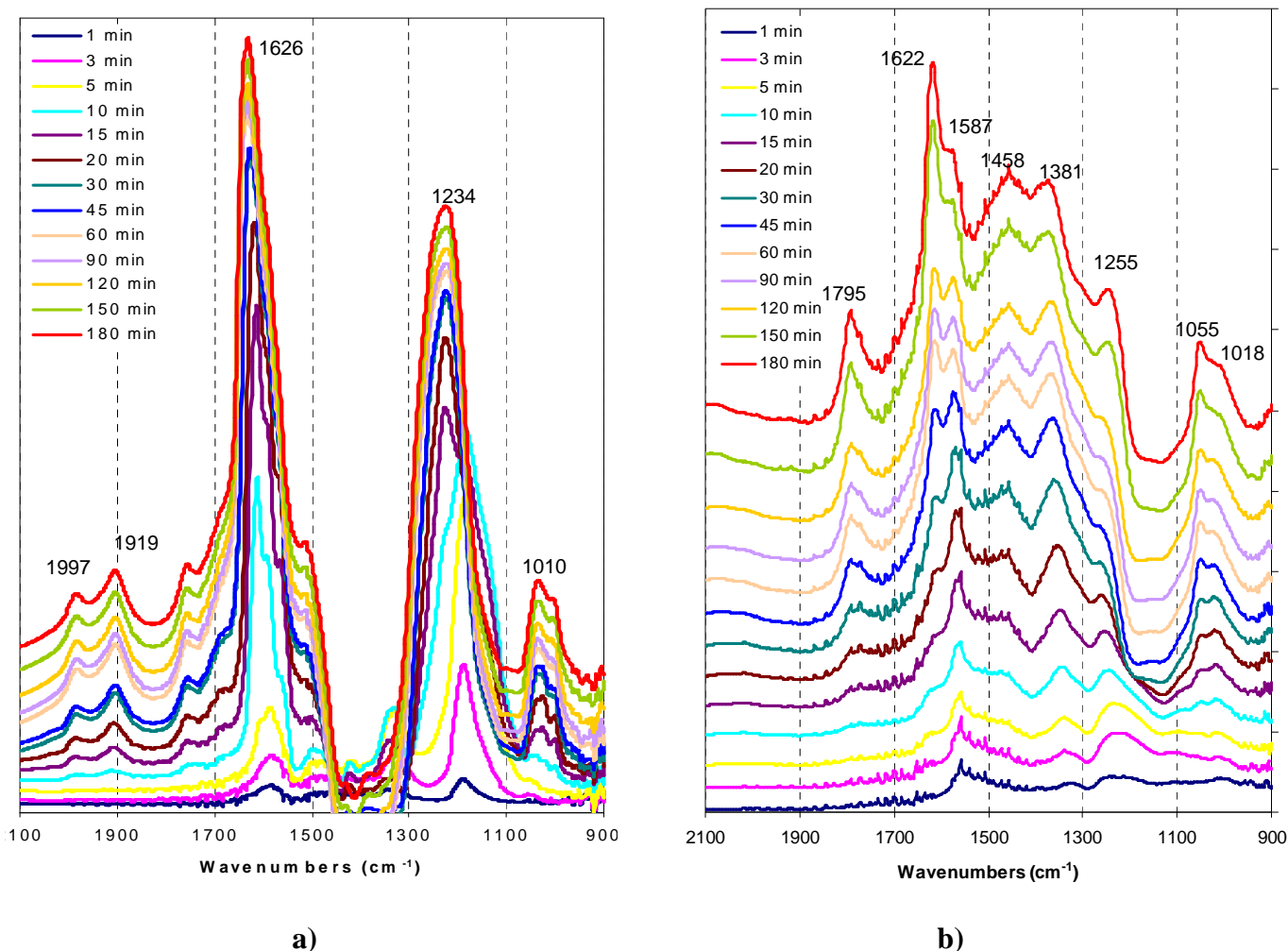
Figure 13 - NO$_X$ adsorption at 200°C in a flow of 800ppm of NO + 20% of O$_2$ in He for **(a)** ZrO$_2$, **(b)** 20%CaO/ZrO$_2$.

After some minutes the nitrates start to form on the surface of the catalyst as seen in Figure 13. All the spectra are not presented for sake of brevity, but are reported in the Appendix D2. In the following table the band positions and the corresponding structures are summarized.

Table 15 - Reported wavenumbers of adsorbed NO_X species observed on Ca, Sr, La oxide and ZrO_2 and their corresponding structure [51].

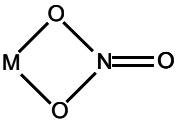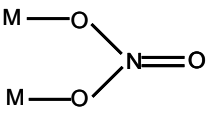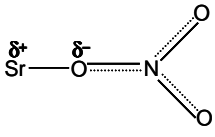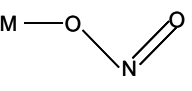| NO_X species	Structure	Vibration	Band position, cm^{-1}
Bidentate nitrate		$\nu\nu(NO_2, as)$	1200-1310
		$\nu\nu(N=O)$	1500-1630
		$\nu\nu(NO_2, s)$	1003-1040
Bridged nitrate		$\nu\nu(NO_2, as)$	1200-1260
		$\nu\nu(N=O)$	1590-1660
		$\nu\nu(NO_2, s)$	1000-1030
Nitrosyl	Sr—O N$^-$ or Sr—NO$^-$	$\nu\nu(NO)$	1103-1810
Ionic nitrate		$\nu\nu(NO_3, as)$	1400-1460
		Partially overlapped	1300-1360
		$\nu\nu(NO_3, s)$	1038
Nitrito		$\nu\nu(N=O)$	1400-1485
		$\nu\nu(NO)$	1050-1100
		$\delta\delta ONO$	820-840

Analyzing figure 13 (a and b) and table 15 it is possible to observe that after some minutes some bands start to increase intensity in both samples at around 1620-1630, 1230-1250 and 1010-1020 cm^{-1} which can be associated with the formation of bridged or bidentate nitrates. Over the time, these bands increase intensity continuously until saturation with nitrates is reached. It is also seen that after 30-45 minutes all the nitrate peaks become effectively visible.

It is impossible to differentiate bridged or bidentate nitrates because they have characteristic adsorption bands in the same regions. But for the ZrO_2 sample it is probable that the predominant species are the bridge nitrates, because the structure is more stable than bidentate nitrate species. The bands for CaO/ZrO_2 at 1381, 1458, 1587 and 1055 cm^{-1} can be assigned to the ionic nitrates, since they appear only for the catalyst with metal nitrates. Therefore, these bands are typical when the metal nitrate is added.

Finally the bands around 1780-1795 cm^{-1} can be assigned to nitrosyl species and can be correlated to the presence of metal on the surface. The other systems showed similar spectra like calcium, but are not presented for sake of brevity (Appendix D2). However it should be noticed that the rate of development of the peaks between samples is different. As example, in zirconia the bands around 1630 and 1240 increase intensity within few minutes, while for the other systems it takes at least 30-45 minutes.

In the third phase - ***desorption in air*** - the samples were treated again with the same flow and temperature conditions as for decomposition of bulk nitrates. This means, temperature increase from 200°C to 600°C with a 20 minutes isotherm. As expected, the surface nitrates that were formed during adsorption start to decompose as temperature increase. Figure 17 shows the desorption of nitrate compounds for the 20%CaO/ZrO$_2$ in air:
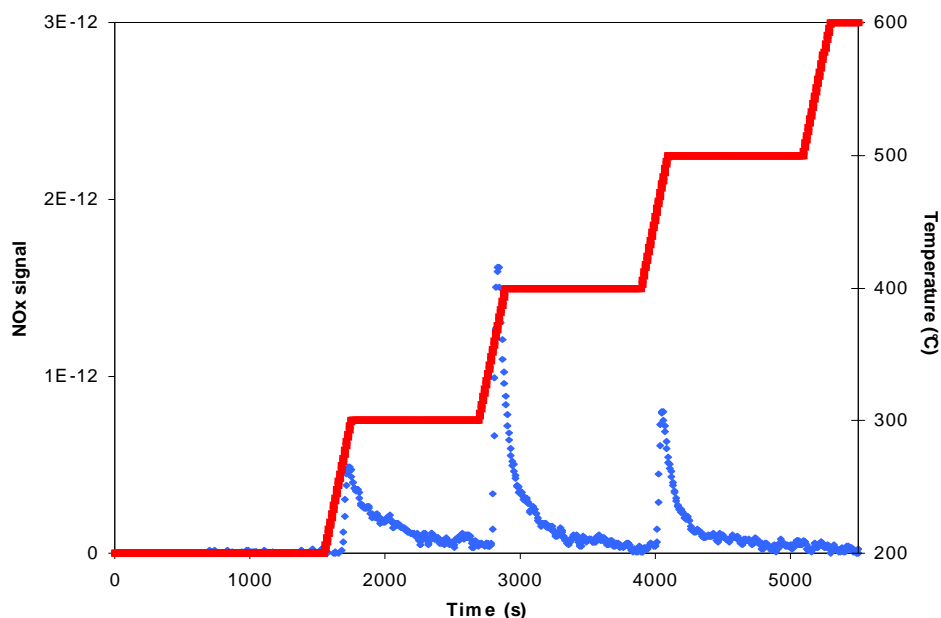
Figure 14 **-** Desorption in air for 20%Ca(NO$_3$)$_2$ /ZrO$_2$ sample with increasing of temperature from 200°C to 600°C with a 100°C steps, heating rate of 1800°C/h followed by an isotherm of 20 min at each temperature and in a flow of 30 ml/min of air (red-T; blue-NO$_X$ signal).

During desorption, the nitrates reach the maximum release of NO at lower temperatures then in the decomposition phase. In this case they are released between 300°C and 400°C. From the area under this curve it is possible to calculate the actual NO$_X$ storage capacity of the system according to equation **(10)**.

Figure 15 represents the spectrum that was collected by increasing the temperature from 200°C and 600°C during the desorption step.

a)   **b)**
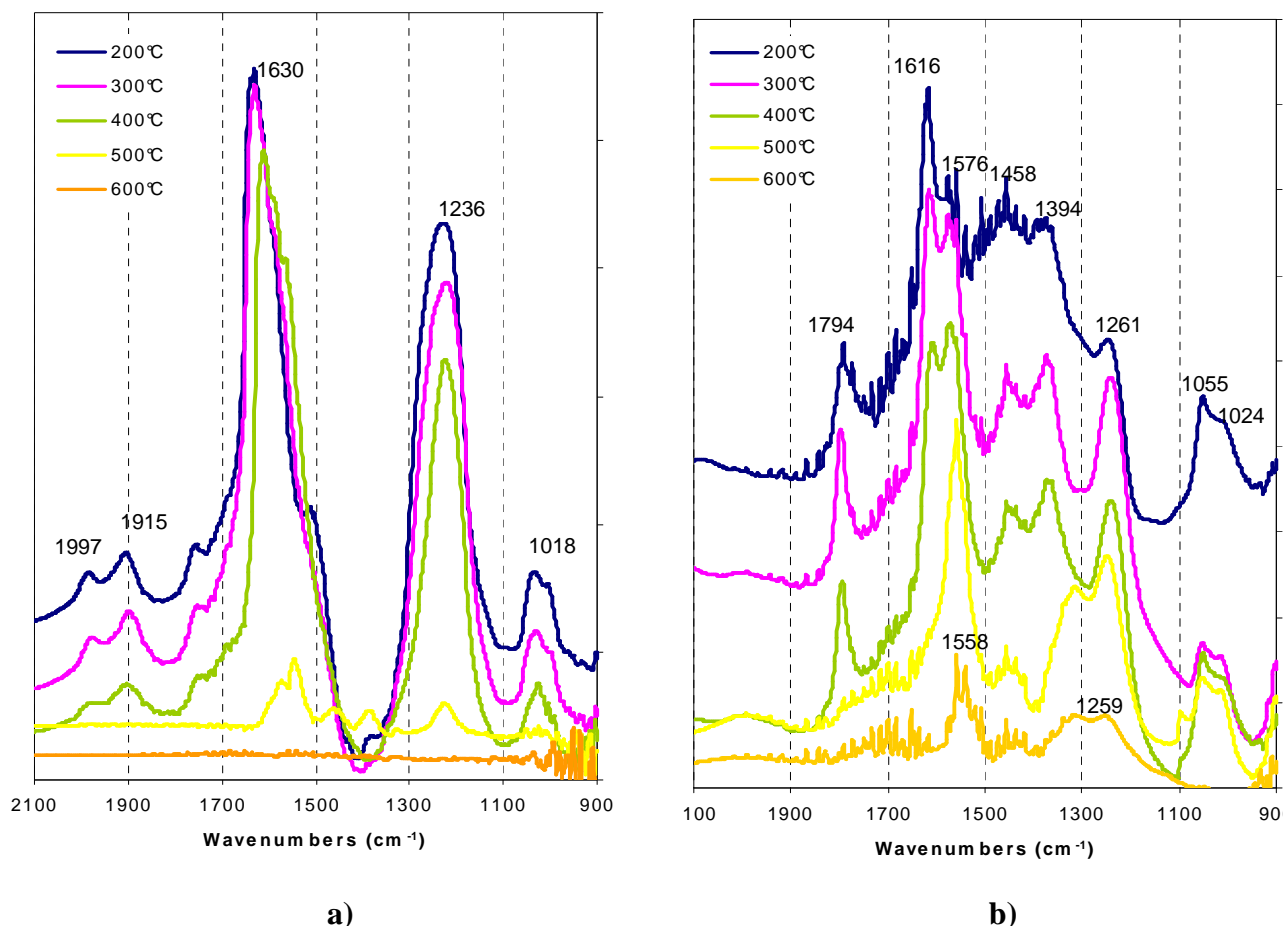
Figure 15 - Desorption spectra for **a)** ZrO_2; **b)** 20%CaO/ZrO_2. Conditions: heating rate of 1800°C/h followed by an isotherm of 20 min at each temperature in a flow of 30 ml/min of O_2.

The intensity of the bands decrease as temperature increases, and at 600°C most of the bands disappear (in ZrO_2 they all disappear), indicating almost complete decomposition of stored nitrates. However some minor bands at 1259 and 1558 cm^{-1}, characteristic for bidentate or ionic nitrate species, still remain, particularly in $Ca(NO_3)_2/ZrO_2$ and $Sr(NO_3)_2/ZrO_2$.

Similar NO storage-release cycles were performed for Sr and La-based systems and the results are summarized in Table 16, while the spectra themselves are omitted and can be found in Appendix D2.

Table 16 – NO_X Storage Capacities of different samples obtained from FTIR-MS results.

Sample	Relative NO_X Storage Capacity (%)	Measured NO_X Storage Capacity (µmol/g)	Absolute NO_X Storage Capacity (µmol/g)	NO_X released between 200°C and 500°C (%)
ZrO_2	-	-	33	82.7
20% $Ca(NO_3)_2$-ZrO_2	71.5	675	944	96.9
20% $Sr(NO_3)_2$-ZrO_2	34.4	325	945	76.9
20% $La(NO_3)_2$-ZrO_2	26.8	327	1258	71.1

Table 16 shows that the NO_X storage capacity obtained in FTIR-MS is lower than for the same samples studied with the TPD-MS. In TPD-MS the samples have approximately 25% higher storage capacity. That happens because the reactor "type" used in TPD is more suited for adsorption studies then the drift cell in the FTIR, and the concentrations of NO_X used during the adsorption step were also higher.

It should be also noticed that for adsorption in FTIR-MS is used NO, and not NO_2 as in the TPD. Therefore this could be also a reason for the high storage capacity in the TPD-MS.

5.5 Pre-treatment

To study the influence of the pre-treatment on the storage capacity, we chose $20\%Sr(NO_3)_2+1\%Pt/ZrO_2$ because it is the catalyst with best soot oxidation performance and a good storage capacity. Approximately 200 mg of sample (previously diluted with SiC in ratio of 1:6 and packed between two quartz wool plugs) was used. Three different preactivation procedures were applied:

1st Experiment (He) – In the first stage (decomposition of the bulk nitrates) the sample was heated from room temperature to 600°C with a heating rate of 10°C/min, in a flow of 50 ml/min of He and then dwell for 150 minutes at 600°C. The second stage (adsorption) was done under the same conditions as the normal storage-release cycles (10ml/min of 2.5% of NO_2 in He during 30 minutes). In the third stage (desorption) the sample was heated from room temperature to 600°C with a heating rate of 10°C/min, in a flow of 50 ml/min of He and then dwell for 20 minutes at 600°C.

2nd Experiment (Air) – This pretreatment was exactly the same as the first, but instead of pure helium, the total flow was 10 ml/min of O_2 and 40 ml/min of He.

3rd Experiment (Air / 5% H_2 in Ar) - In the first stage (decomposition of the bulk nitrates) the sample was heated from room temperature to 600°C with a heating rate of 10°C/min, in a flow of 10 ml/min of O_2 and 40 ml/min of He and then dwell for 20 minutes at 600°C. At 600°C the sample was pretreated with 2.5ml/min of H_2 and 47.5ml/min of Ar during 150 min. The second stage (adsorption) was done under the same conditions as the normal storage-release cycles. In the third stage (desorption) the sample was heated from room temperature to 600°C with a heating rate of 10°C/min, in a flow of 10 ml/min of O_2 and 40 ml/min of He and then dwell for 20 minutes at 600°C.

Table 17 shows the results obtained for each pre-treatment procedure:

Table 17 – NO$_X$ Storage Capacities for 20%Sr(NO$_3$)$_2$+1%Pt/ZrO$_2$ obtained from TPD-MS for three different pre-treatment procedures.

Pre-Treatment Procedures	Relative NO$_X$ Storage Capacity (%)	Measured NO$_X$ Storage Capacity (μmol/g)	Absolute NO$_X$ Storage Capacity (μmol/g)	NO$_X$ released between 200°C and 500°C (%)
He	51.4	486	945	60.5
Air	73.5	695	945	60.8
Air / 5%H$_2$ in Ar	85.7	810	945	81.5

5.6 Final optimization of the catalyst

Until this point, all the samples were impregnated with platinum using 1g of metal nitrate supported on zirconia and then impregnated with 0.8ml of Pt-containing solution – we can call it the "standard" method. In order to improve the soot oxidation performance (with air) the final catalyst (20%Sr(NO$_3$)$_2$+1%Pt/ZrO$_2$) was impregnated with platinum by two additional preparation/activation procedures:

1. The Pt solution (0.8ml) was added to the Sr nitrate solution (0.8ml) and then this mixture was used to impregnate the ZrO$_2$ (0.8g). Afterwards the sample was dried for two hours at 120°C.

2. The support (0.8g) was impregnated with Pt solution (0.8ml). After impregnation, the sample was dried for two hours at 120°C. On the next day the sample was calcined for five hours at 500°C. Afterwards Sr nitrate solution (0.8ml) was added and in the following day the sample was dried for two hours at 120°C.

Table 18 shows the results obtained for each preparation method.

Table 18 – Temperature of the max peak of CO$_2$, 20% and 50% conversion of soot, nitrate decomposition peak and soot conversion at 500°C and the selectivity obtained for three different procedures.

Methods	T$_{max\ peak}$ (°C)	T$_{20\%\ conv}$ (°C)	T$_{50\%\ conv}$ (°C)	T$_{nitrate\ peak}$ (°C)	Conv$_{500°C}$ (%)	Selectivity (%)
Standard	623	487	581	480	24.1	91.9
1	626	513	594	480	16.1	93.6
2	615	499	582	474	20.3	93.0

5.7 Stability Testing

Finally the stability of the final system – $Sr(NO_3)_2$ +1%Pt/ZrO_2 was tested in multiple NO_X storage/release cycles. For that, the same sample was submitted to 8 storage-release cycles in TPD-MS using the same conditions already mentioned in section 5.4. This means that the catalyst was submitted to decomposition of the bulk nitrates to know how much NO_X are stored in the beginning. Then adsorption was performed with 2.5% NO_2 in He at 200°C and finally desorption of the nitrates in air. These last two steps were repeated 8 times. Table 19 gives the obtained results:

Table 19 - Stability Testing of $Sr(NO_3)_2$+1%Pt/ZrO_2 obtained from TPD-MS.

Number of Cycle	Relative NO_X Storage Capacity (%)	Measured NO_X Storage Capacity (µmol/g)	Absolute NO_X Storage Capacity (µmol/g)
1	60.9	576	945
2	57.8	546	945
3	59.5	562	945
4	58.5	552	945
5	60.5	572	945
6	59.1	559	945
7	58.6	554	945
8	59.7	564	945

It is clearly seen that the catalyst shows good stability and the differences between the results achieved are within the error of the equipment.

5.8 Comparison between ZrO_2-supported systems with Al_2O_3

To complete the final goal of the thesis the data obtained for the ZrO_2 supported system it were compared with those of Al_2O_3 system, obtained by Arkady Kustov. All data were obtained following the same procedures that were previous mentioned in the Experimental section (soot-catalyst-SiC ratio was 1:20:120).

Table 20 shows the results obtained by TGA and by TPD-MS for Mg, Ca, Sr and Ba nitrates supported in Al_2O_3.

Table 20 – Temperature of nitrate decomposition (TGA), temperature of the 20% conversion of soot and selectivity to CO_2 (TPD-MS).

Sample	$T_{nitrate\ dec}$ (°C)	$T_{20\%\ conv}$ (°C)	Selectivity (%)
Soot +Al_2O_3	642	584	88
Soot+20%$Mg(NO_3)_2$ / Al_2O_3	100-300	530	84
Soot+20%$Ca(NO_3)_2$ / Al_2O_3	300-450	486	81
Soot+20%$Sr(NO_3)_2$ / Al_2O_3	505	509	86
Soot+20%$Ba(NO_3)_2$/ Al_2O_3	610	542	85
Soot+20%$Ca(NO_3)_2$ +1%Pt-Al_2O_3	432	470	92
Soot+20%$Sr(NO_3)_2$ +1%Pt-Al_2O_3	467	484	97
Soot+20%$Ba(NO_3)_2$ +1%Pt-Al_2O_3	512	514	91

NO storage-release cycles were performed using FTIR-MS for the same systems and the results are summarized in Table 21.

Table 21 – NO_X Storage Capacities for different samples obtained from FTIR-MS

Sample	NO_X Storage Capacity (%)	NO_X released between 200°C and 500°C (%)
Soot+20%$Mg(NO_3)_2$ / Al_2O_3	6.1	97
Soot+20%$Ca(NO_3)_2$ / Al_2O_3	24.9	57
Soot+20%$Sr(NO_3)_2$ / Al_2O_3	16.5	34
Soot+20%$Ba(NO_3)_2$/ Al_2O_3	5.7	15

6. Discussion

A system was required for improving soot oxidation in passenger cars. For that reason, NO_X assisted soot oxidation catalyst need to be developed, that later could be implemented in a catalytic filter. In order to develop such catalyst the capacity of several materials based on zirconia support to store NO_X at temperatures below 300°C as nitrates and release it at the temperature range of regeneration and also high temperature soot oxidation was studied.

For this purpose Mg, Ca, Sr Ba-systems and La, Ce and Pr-systems were prepared. These specific components were selected because alkali-earth and rare earth metals oxides with Zr are known to form nitrates upon reaction with NO_X.

To increase the oxidation function 1% platinum was added to the systems that showed better soot conversion and NO_X storage capacity efficiency. To study the stability of the best catalyst 8 storage/release cycles were performed. Different pre-treatment procedures were studied to

determine their influence on the storage capacity and different methods of producing the catalyst were also subject to study, in order to evaluate their influence on soot oxidation.

6.1 Temperature of decomposition of the bulk nitrates

For the practical application in soot trap the storage compound should release nitrates at temperatures above 400°C. According to the TGA data (see figure 8 and 9), nitrates are decomposed too early on Mg and Ce-based systems (before 200°C) and consequently most of the nitrates will be released before regeneration, during normal engine conditions. In the case of Ba system nitrates are decomposed only at around 600°C, which seems rather unpractical, since uncatalyzed soot oxidation also starts in this region and there will be no benefit in the temperature of the soot oxidation. Of course, the Ba-based system still should not be discarded, because the presence of the driving force (reducing atmosphere) should facilitate the decomposition of nitrates. Nevertheless based on the temperatures of nitrates decomposition, Sr, Ca, La and Pr-based systems look more promising since they are decomposed at temperatures between 350-550°C. But these are bulk nitrates, and we are of course more interested in actual stored nitrates; therefore the next step is to study all these systems in storage-release cycles and in soot oxidation.

6.2 Effect of different catalytic systems on soot oxidation

In the case of the TPD set up, a 0.5:1 N/C ratio was used. For uncatalysed soot oxidation (no stored nitrates present at the system) the temperatures of 20% and 50% soot conversion were quite high, around 580°C and 634°C respectively. This way, only 6.7% of soot is converted at 500°C, which increases the importance of the use of metal nitrates. After introduction of stored nitrates into the system, the temperature of soot oxidation decreases quite significantly, except in the case of cerium nitrate (conversions similar to uncatalysed soot conversion).

Analysing the different catalytic systems (table 8) it is possible to observe that in the case of 20% $Mg(NO_3)_2/ZrO_2$ and 20%$Ce(NO_3)_3/ZrO_2$ the nitrates start to decompose too early. As a result these systems may not be considered as good for NO_X assisted soot oxidation. However, stored nitrates could decompose at higher temperature then model. So, it is not possible to affirm that they are excluded.

Analysing other systems, it is possible to see that best performance is achieved with 20%$Ca(NO_3)_2/ZrO_2$, 20%$Sr(NO_3)_2/ZrO_2$, 20%$Pr(NO_3)_3/ZrO_2$ and 20%$La(NO_3)_3/ZrO_2$ systems, especially in the case of Pr-based system. With La nitrate the temperature for 20% soot conversion decreases 74°C in comparison with uncatalysed soot oxidation. The amount of soot converted before 500°C is also quite high, around 19%, while other Ca, Sr and La give values

around 16%, 13% and 17% respectively. The $20\%Ba(NO_3)_2/ZrO_2$ sample shows lower conversion (9.6%), perhaps because the nitrates start to decompose only above 420°C and the NO peak is above 560°C; at this temperature NO_X mainly exist as NO that is not so active for soot oxidation. Nevertheless, based on the soot oxidation, Ca, La and Pr-based systems look more capable. But this is only one part of the problem and we are of course interested in storing nitrates under normal driving conditions, therefore the next step is to study all these systems in storage-release cycles. Data for the TPD-MS are summarized in Table 8.

Analysing all the soot oxidation data in Appendix B1, two mechanisms of soot oxidation can be identified: NO_X assisted soot oxidation at low temperatures, coinciding with the temperatures of the nitrates decomposition; and high-temperature uncatalysed soot oxidation with O_2, which prevails when all nitrates are already decomposed. Since the ratio between the amounts of available NO_X and soot are quite low the decomposition of nitrates does not provide enough NO_2 to oxidize all soot. Also, the thermodynamic stability of NO_2 at high temperatures is quite low, and NO_X mainly exists as NO, which is inactive for soot oxidation.

In the case of the Six-flow reactor the N/C ratio is only around 0.1:1 versus 0.5:1 in TPD experiments, for that reason, the effect of nitrates was not as prominent as in the case of TPD experiments. In the first experiment (table 11), the results do not show large differences between the different systems (at maximum 10°C in soot conversion). Comparing the rare earth metals with the alkali-earth metals that have smaller amounts of nitrates, the results are the same. This can be explained by the low ratio of nitrates that were used in the experiments and by the slow heating ramping rate. When platinum was added (experiment 2) the selectivity to CO_2 and the conversion of soot increased, which can be taken as a trend. Also, in experiment 3 and 4, the addition of platinum increased the conversion of soot.

6.3 Effect of different catalytic systems on NO_X storage capacity

The results of storage/release cycles obtained by TPD-MS (summarized in Table 10) show that Ba, Ce, La and Pr-based systems have the lowest NO_X storage capacity (39.7%, 24.2%, 45.3% and 37% respectively).

The available storage capacity increases on going from Ba to Ca, which can be related with the difference in the availability of the storage component and with the decrease of the basicity of the cation used. The Mg based-system falls out of general trend probably due to the fact that some of the stored nitrates are decomposed at storage conditions (200°C). The Ce based-system has the same problem as Mg.

The Ca and Sr-based systems achieved good storage capacity, 91% and 61% respectively. However, only 36% and 25% of the NO is released between 200°C and 500°C respectively. So the storage capacity is far from being optimal, indicating that most storage components does not participate in nitrates storage. To increase the share of NO_X released between 200°C and 500°C: **(1)** an oxidation function can be added and **(2)** different pre-treating conditions can be applied, which will be discussed further.

Storage capacity was also studied in FTIR-MS using the drift cell. According to the results most of the NO_X is adsorbed within first 30-45 minutes. Also the samples studied (ZrO_2, Ca, Sr and La-based systems) show some bands of major intensity at around 1624, 1234 and 1012 cm^{-1} which can be associated with the formation of bridged or bidentate nitrates. The bands at around 1458, and 1050 cm^{-1} can be assigned to the addition of the metal nitrate on the ZrO_2 (ionic nitrates). Band at 1780-1790 cm^{-1} can be assigned to nitrosyl species and can be correlated to the presence of metal (Ca, Sr and La) on the surface. Analyzing table 16 is possible to observe that the NO_X storage capacities obtained in FTIR-MS show similar trends as those obtained in TPD-MS. However, the storage capacity in FTIR-MS is 25% lower for the same catalysts used. That happens because the reactor "type" used in TPD is better suited for adsorption studies than the drift cell in FTIR, and the concentrations of NO_X used during adsorption step were also higher.

6.4 Effect of Pt addition in different catalytic systems on soot oxidation and on storage capacity

TPD-MS experiments showed that only 36% and 25%, of the NO is released between 200°C and 500°C for Ca and Sr based-system, respectively. This low efficiency of nitrates utilization can be improved by recycling NO to NO_2 during the reaction. Therefore platinum was added to the catalyst formulation. The presence of platinum on the surface of the catalyst influence soot oxidation since it can increase the oxidation rate (NO to NO_2). Therefore by adding platinum, all samples achieved higher conversions at the same temperature, and of course higher selectivities to CO_2. Sr based-system showed higher conversions (24.1% at 500°C), while La had the lowest temperature at 20% of conversion (483°C).

At the same time, by studying storage/release cycles, it was found that Pt has almost no effect on NO_X storage capacity (Table 10), but decreases the temperature of nitrates decomposition/desorption by at least 50°C, and in the case of Sr based-system the decrease is 180°C. As a result, the percentage of NO released between 200°C and 500°C is increased by at least 20%, and in the case of Sr-based system increased from 25% (without Pt) to 52% (with Pt).

Significant improvement in terms of catalytic activity as well as selectivity was observed when Pt was added to the storage component (Table 10).

Combining both platinum and storage component allows us to lower the temperature of 20% conversion by more than 90°C, compared to uncatalysed soot oxidation. As shown by TPD experiments soot oxidation with Sr-based system and the amount of soot removed before 500°C increases from 6% to more than 24%, which can be considered as a great progress.

For six-flow reactor experiments (second experiment) the results clearly show that by introducing platinum, the selectivity of soot conversion to CO_2 is increased significantly, but has little impact on the amount of soot converted before 500°C (3-4% increase). In the third experiment, uncatalysed soot oxidation is compared with catalysed soot oxidation with and without platinum. The results show that with stored nitrates the temperature of 20% soot conversion decreased (3-5°C), but not so significantly as could be expected, and the amount of soot converted before 500°C also decreased slightly, comparing $20\%Ca(NO_3)_2/ZrO_2$ with ZrO_2. This difference may be due to the error of the equipment. In the three 6-flow experiments it is possible to notice that the temperatures of 20% conversion and 50% conversion are quite similar for all the catalysts, except in the case of ZrO_2 (uncatalysed reaction) that is 5-10°C higher.

The drawback of the systems studied is the significant amount of soot that is oxidized through the non-catalyzed route, mainly because the concentration of NO_X during regeneration is not sufficiently high. To achieve complete soot oxidation at low temperature, the ratio between catalyst and soot should be increased even further (to obtain N/C ratios around 1 and higher).

6.5 Effect of different after-treatment techniques on NO_X storage capacity

Since the storage capacity is far from being optimal, indicating that most of storage component does not participate in nitrates storage, we tried three different preactivation procedures. To study the influence of the pre-treatment in the storage capacity, we chose the catalyst with better soot oxidation performance and a good storage capacity (around 62%) - $Sr(NO_3)_2+1\%Pt/ZrO_2$.

In the first procedure the sample was pretreated in helium at 600°C and the storage capacity was around 54%. The second procedure was pretreating in air, which led to an increase of the amount of stored NO_X up to 74%. The most pronounced increase of the storage capacity was obtained after pretreating in reducing atmosphere (air + 5% H_2 in argon), giving storage capacity of more than 85% and the amount of NO_X desorbed between 200 and 500°C also increased significantly (from 60 to 82%). The results achieved between different pretreating conditions can

be related with redispersion of the storage component. This means that H_2 allows a higher dispersion, resulting in more available storage component for NO_X storage. It should be noticed that it is unknown if the dispersion achieved with H_2 is stable after the first cycle. For that reason, repetitive storage release cycles using 5%H_2 in Ar should be studied in future.

The last procedure showed higher storage capacity because we assume [49] that H_2 increases the storage capacity. However this would never be possible in a real engine because there is no H_2 in diesel exhaust; as a result this technology cannot be applied to our system. Nevertheless, the catalyst can be pretreated before putting it into the engine. If dispersion is higher, then storage capacity would also be higher. For that reason, it could work.

6.6 Effect of different preparation and activation procedures on soot oxidation - final optimization of the catalyst

To improve the soot oxidation performance (with air), the final catalyst - 20%$Sr(NO_3)_2$ +1%Pt/ZrO_2 was impregnated with platinum by other two preparation/activation procedures, as was explained in detail in section 5.6.

By analyzing table 18 it can be seen that in all procedures the selectivity is increased after introduction of Pt, as expected. The first procedure resulted in lower soot conversions (16.1%) at 500°C, while the second route led to 20.3% soot conversion. Since in the first method the Pt and Sr solution are mixed before impregnation, it is possible that the majority of the Sr layers formed during the impregnation are above platinum. In that way there is less recycling of NO to NO_2 to oxidize soot because the Pt sites are not so accessible.

In the second method the sample was calcined at 500°C forming medium size clusters of Pt on the catalyst that increase the recycling of NO to NO_2, however bigger and enough clusters were not formed so that conversion of soot at 500°C (20.3%) could be higher compared with the "standard" procedure (24.1%). Bigger clusters have higher specific activities than smaller ones (<50nm) meaning that larger clusters are more active (soot catalytic reactions are size dependent [12][50]).This does not mean that the "standard" method is the best, because it is known in literature (Xue et al [50]) that if the temperature of calcination is increased until 700°C [12], more and bigger clusters (>100nm) are formed that increase the recycling of NO to NO_2 and as consequence increase soot oxidation rate.

6.7 Study of the stability of the optimal catalyst

In the end we have tested the stability of the final system – $Sr(NO_3)_2 + 1\%Pt/ZrO_2$. For that, the same sample was submitted to 8 storage-release cycles in TPD-MS using the conditions already mentioned in section 5.7.

It is clearly seen that the catalyst shows good stability and the differences between the results achieved are within the error of the experiment. The following figure exemplifies the good stability of the system.
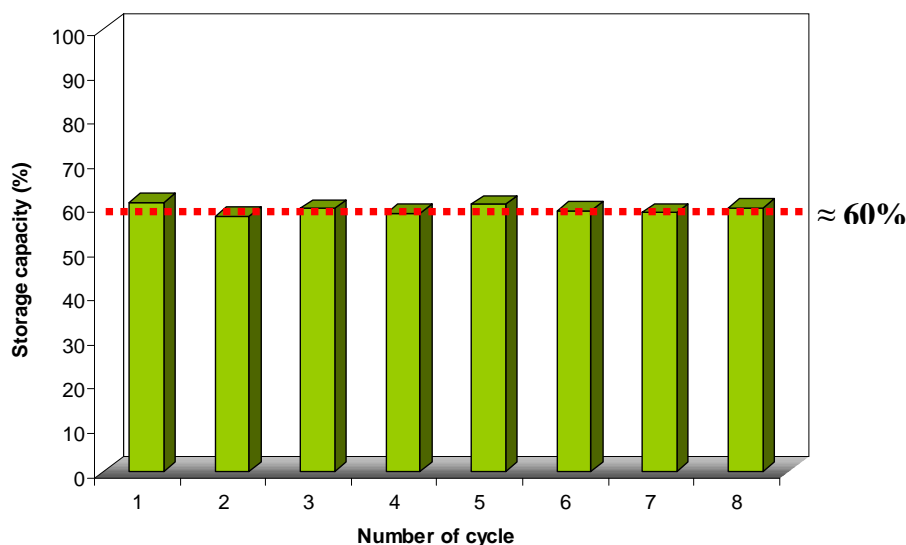

Figure 16 – Stability testing for $20\%Sr(NO_3)_2 + 1\%Pt/ZrO_2$.

6.8 Comparison between ZrO$_2$-supported systems with Al$_2$O$_3$

Analyzing tables 8 and 9, and comparing then with table 20, a similar trend is observed between the systems. When Pt is added, selectivity and soot conversion increase in all samples. Sr based-systems show similar temperatures of 20% conversion for soot – 483°C (Al_2O_3) versus 487°C (ZrO_2). However, comparing Ca-based systems for both supports, the temperature of soot conversion is approximately 20°C lower using alumina support. It is concluded that alumina as the same or better conversion of soot at the same temperature.

Comparing the results in table 16 with table 21 (FTIR-MS) it is possible to say for the same sample (for example Ca), that the zirconia support can store more nitrates – 71% (ZrO_2) versus 25% (Al_2O_3). Also, the NO_X released between 200°C and 500°C is smaller. This means that zirconia has better potential for NO_X storage then alumina. But if zirconia can store more nitrates it should have higher soot oxidation rates. This does not happen because maybe in alumina the efficiency of NO_X utilization is higher. Also has a higher surface area and for soot oxidation the surface area is very important. With higher surface area the contact between the soot and the catalyst is increased favoring soot oxidation.

6.9 Comparison between ZrO$_2$-supported systems (Sr(NO$_3$)$_2$)

Data obtained in this work were compared to the data obtained for ZrO$_2$ supported system by Francesca Ricciardi [47]. All data were obtained following the same procedures that were previous mentioned in the Experimental section (soot-catalyst-SiC ratio was 1:20:120).

Analyzing tables 8 and 9 and table 22, a similar trend is observed between the systems. When Pt is added selectivity and soot conversion increase. The system shows similar temperatures of 20% conversion for soot – 487°C versus 475°C. However comparing the conversion at 500°C, her system achieved better results – 24% versus 32%. The reasons could be the error associated with the equipment and the person. Everybody work differently, therefore could be possible that small differences could exist while preparing the catalyst or mixing it with soot. For example, the time spent mixing the soot with the catalyst can be different. This can be an important factor, because if soot is mixed for more time, the contact between soot and catalyst is increased and this can favor soot oxidation.

Comparing the results in table 16 with table 22 is possible to state that for both samples the NO$_X$ storage is about the same – 31.4% versus 34.1%. So both systems show similar trends.

Table 22 – Temperature of nitrate decomposition (TGA), temperature of the 20% conversion of soot, conversion of soot at 500°C, selectivity to CO$_2$ and NO$_X$ storage capacity (FTIR-MS).

Sample	T$_{nitrate\ dec}$ (°C)	T$_{20\%\ conv}$ (°C)	Conv$_{500°C}$ (%)	Selectivity (%)	NO$_X$ Storage Capacity (%)
Soot+20%Sr(NO$_3$)$_2$ / ZrO$_2$	530	508	16.7	79	33.8
Soot+20%Sr(NO$_3$)$_2$ +1%Pt-ZrO$_2$	470	475	32.0	92	31.4

7. Conclusions

Based in all data obtained it is concluded there are two mechanisms of soot oxidation after introduction of stored nitrates: NO$_X$ assisted soot oxidation at low temperatures, coinciding with the temperatures of the nitrates decomposition and high-temperature uncatalysed soot oxidation with O$_2$ which prevails when all nitrates are already decomposed. Introduction of stored nitrates into the system decreases the starting temperature of soot oxidation more than 70°C (La system) in comparison with uncatalysed soot oxidation. In Mg and Ce-based systems the nitrates start to decompose too early, meaning that they cannot be considered good assisted soot oxidation systems and are excluded from further investigations. The effect of nitrates was not as prominent

in the Six-flow reactor experiments because the N/C ratio was only around 0.1:1 versus 0.5:1 in TPD experiments and the heating rate used do not favour NO_X assisted soot oxidation.

The best NO_X storage capacity was achieved for Ca and Sr-based systems, 91% and 61% respectively in TPD-MS. But the storage system is not optimal since NO released between 200°C and 500°C was too low. NO_X storage capacity obtained in FTIR-MS shows similar trends as those obtained in the TPD-MS. However, in the FTIR-MS storage capacity is 25% lower for the same catalysts used because the reactor "type" used in TPD is a more suited for adsorption studies than the drift cell in the FTIR and is used NO and not NO_2 .

The combination of bulk nitrates and Pt increases soot oxidation even further, as well as the selectivity of soot conversion to CO_2 by oxidizing formed CO. Sr based-system showed the best conversion - 24.1% at 500°C, while La showed the lowest temperature of 20% soot conversion - 483°C (90°C less than uncatalysed soot oxidation). Significant amount of soot is still oxidized through non-catalyzed route, mainly because the concentration of NO_X during regeneration is not sufficiently high. To achieve complete soot oxidation at low temperature the ratio between catalyst and soot should be increased even further. Pt has almost no effect on NO_X storage capacity but decreases the temperature of nitrates decomposition/desorption by at least 50°C, and in the case of Sr based-system by 180°C.

Sr based-system showed promising soot oxidation activities and good storage capacity. For that reason this system was chosen as the final catalyst to improve. After pretreating the Sr-based catalyst in reducing atmosphere (air + 5% H_2 in argon), storage capacity increased to more than 85% and the amount of NO_X desorbed between 200 and 500°C also increased significantly (82% of all NO_X in the sample is released in this range).

To improve the soot oxidation performance (with air) the final catalyst was impregnated with platinum by other two preparation/activation procedures. However by the "standard" method better results were achieved, indicating the importance of Pt location on top of Sr-layers.

The final catalyst was submitted to 8 storage-release cycles in TPD-MS and demonstrated good stability. Average of 60% storage capacity was achieved. The differences between the results attained are within the error of the experiment.

Finally is concluded that soot oxidation data obtained for the ZrO_2 supported system follow the same trend as for Al_2O_3 system. On the other hand, for the same samples, the zirconia support can store more nitrates – 71 % (ZrO_2) versus 25% (Al_2O_3) in case of Ca. The amount of NO_X released between 200°C and 500°C is also higher in the case of the zirconia support. Alumina can be considered a better soot oxidation system because has a surface area higher than zirconia and as a result the contact between the soot and the catalyst is increased favoring soot oxidation.

8. Recommendations for future work

♦ To achieve complete soot oxidation at low temperature the ratio between catalyst and soot should be increased even further in the six flow reactor set-up (to obtain N/C ratios around 1 and higher).

♦ Stability of the dispersion achieved with H_2 is unknown after the first cycle. For that reason multiple storage release cycles using $5\% H_2$ in Ar should be studied.

♦ Is recommendable to use the additional activation method/procedure to investigate if calcination at higher temperatures, for example at 700°C, forms bigger clusters of platinum so that could improve the conversion of soot at 500°C compared with the "standard" procedure.

♦ Apply other storage component in combination with $Sr(NO_3)_2/ZrO_2$, such as Ca. This mean to study a bimetallic catalyst.

♦ Study the influence of the metals concentration (Ca and Sr as a bimetallic catalyst) on the NO_X storage capacity and assisted soot oxidation.

♦ Improve the efficiency of NO_X utilization in ZrO_2.

♦ Try to find a support with a higher surface area and NO_X storage capacity than Al_2O_3.

9. References

[1] B.A.A.L. van Setten, *Development of a Liquid Catalyst for Diesel Soot Oxidation*, PhD Thesis, Delft University of Technology (2001), 1-5.

[2] B.R. Stanmore, J.F. Brilhac, P. Gilot, *Carbon* 39 (2001) 2247.

[3] K. Krishna, M.Makkee, *Catalysis Today,* 114 (2006), 48-56.

[4] V.G. Milt, C.A. Querini, E.E. Miro and M.A. Ulla, *J. Catal.* 220 (2003), 424.

[5] F. Jacquot, V. Logie, J.F. Brilhac, P. Gilot, *Carbon* 40 (2002), 335-343.

[6] G. Mul, W. Zhu, F. Kapteijn, J.A Moulijn,. *Appl. Catal. B: Environ* 17 (1998), 205-220.

[7] http://www.auto.howstuffworks.com accessed in February 2008.

[8] J.P.A. Neeft, M. Makkee, and J.A. Moulijn, *Diesel particulate emission control*, Fuel Process Technology (1996), 3-30.

[9] http://www.cbs.nl/ , accessed in February 2008.

[10] I. Atribak, I.Such-Basanez, A. Bueno-Lopez and A.Garcia. *J. Catal* 250 (2007), 75.

[11] S.J. Jelles, M.Makkee, J.A. Moulijn, G.J.K. Acres, J.D. Peter Hoblyn, Diesel particulate control. *Application of an activated particulate trap in combination with fuel additives at an ultra low dose rate*, (1999).

[12] S.J. Jelles, *Diesel Exhaust after treatment, development of catalytic systems for diesel particulate oxidation*, Ph.D Thesis, Delft University of Technology, (1999), 98 and 137-139.

[13] A. Farleigh and L. Kaplan, *Danger of Diesel*, U.S. Public Interest Research Group Education Fund, (2000).

[14] http://www.dieselnet.com/standards/eu/ld.php accessed in February 2008.

[15] A. Setiabudi, *Oxidation of Diesel Soot: towards an optimal catalysed diesel particulate filter*, PhD Thesis, Delft University of Technology (2004), 3-10.

[16] J.P.A. Neeft, M. Makkee, and J.A. Moulijn, *Diesel particulate emission control*, Fuel Process Technology (1996), 34-38.

[17] Health Effects Institute. 1995. Diesel Exhaust: *A Critical Analysis of Emissions, Exposure, and Health Effects* (A Special Report of the Institute's Diesel Working Group). Health Effects Institute, Cambridge, MA.

[18] A. Faiz, C.S. Weaver, and M.P. Walsh, *Air Pollution from Motor Vehicles, Standard and Technology for Controlling Emission,* The World Bank, Washington D.C, (1996) 63.

[19] Health Effects Institute. 1995. Diesel Exhaust: *A Critical Analysis of Emissions, Exposure, and Health Effects* (A Special Report of the Institute's Diesel Working Group). Health Effects Institute, Cambridge, MA.

[20] B. Dernaika, *Catalytic Combustion of Diesel Soot*, Master Thesis, Middle East Technical University, Turkey 2001.

[21] J.P.A Neeft, *Catalytic Oxidation of Soot: Potential for the Reduction of Diesel Particulate emissions*, PhD Thesis, TUDelft 1995.

[22] P. Hawker, N. Myers, G. Hurthwohl, H. Th. Voge, B Bates, L. Magnusson, and P. Bronnenberg, *Experience with a new particle trap technology in Europe*, SAE Paper 970182 (1997).

[23] H. Amariglio and X.Duval *Carbon* 4 (1966) 323-332.

[24] B.J. Cooper and J.E. Thoss, *Role of NO in diesel particulate emission control*, SAE Paper 890404, 1989.

[25] C.Querini, M.Cornaglia, M.A.Ulla, E.E.Miro, *Appl.Catal.B:Environ*. 20 (1999)165-177.

[26] G.Saracco, C.Badini, N.Russo, V.Specchia, *Appl. Catal. B: Environ.* 21 (1999) 233–242.

[27] C. Badini, G. Saracco, V.Serra, V.Specchia, *Appl. Catal. B: Environ*. 18 (1998) 137-150.

[28] J.P.A. Neeft, M. Makkee, J.A. Moulijn, *Chem. Eng. J.* 64 (1996), 295-302.

[29] S.J. Jelles, B.A.A.L. van Setten, M. Makkee, J.A. Moulijn, *Appl. Catal. B: Environ*. 21 (1999) 35-49.

[30] B.A.A.L. van Setten, P. Russo, S.J. Jelles, M. Makkee, P. Ciambelli, J.A. Moulijn, *React. Kinet. Catal*. Lett: 67 (1999) 3.

[31] B.A.A.L. van Setten, S.J. Jelles, M. Makkee, J.A. Moulijn, *Appl. Catal. B: Environ.* 21 (1999) 51.

[32] S.J. Jelles, B.A.A.L. van Setten, M. Makkee, J.A. Moulijn, *Appl. Catal. B: Environ*. 21 (1999) 35-49.

[33] C. Badini, G. Saracco, V. Serra, *Appl. Catal. B: Environ*. 11 (1997), 307-328.

[34] G. Lepperhof, H. Luders, P. Barthe, and J.Lemaire, *Quasi-Continuous particle trap regeneration by cerium-additives*, SAE Paper, 950369 (1995) 91.

[35] www.psa.fr accessed in April 2008.

[36] M. Dhakad, T. Mitshuhashi, S. Rayalu, Pradip Doggali, S. Bakardjiva, J. Subrt, D. Fino, H. Haneda, Nitin Labhsetwar *Catalysis Today* 132 (2008), 188-193.

[37] B.A.A.L. van Setten, S.J. Jelles, M. Makkee, J.A. Moulijn*, Appl. Catal. B: Environ* 21 (1999) 51.

[38] Toyota Patent. European Patent Application no. 0573672A1, 1992.

[39] S. Matsumoto, *Cattech.* 4 (2000), 102.

[40] J. Suzuki and S. Matsumoto, *Topics. Catal.* 28 (2004), 171.

[41] G. Busca, L. Lietti, G. Ramis and F. Berti, *Appl. Catal. B: Environ* 18 (1998), 18.

[42] F. Prinetto, G. Ghiotti, I. Nova, J. *Phys. Chem. B* 105 (2001), 12732-12745.

[43] W.S. Epling, L.E. Campbell, A. Yezerets, N.W. Currier and J.E. Parks II, *Catal. Rev.* 46 (2004) (2), 163.

[44] B. J. Cooper, H. J. Jung, J. E. Thoss, *Treatment of diesel exhaust gases*, U.S. Patent 4,902,487, 1990.

[45] M.J. Illán-Gómez, S. Brandán, A. Linares-Solano and C. Salinas Martínez de Lecea, *Appl. Catal. B:Environ* 25 (2000), 11.

[46] N. Nejar, J.M. García-Cortés, C. Salinas-Martínez de Lecea and M.J. Illán-Gómez**,** *Catal. Comm*, 6 (2005), 263-267.

[47] F. Ricciardi, *Influence of surface area on NO_X storage and high temperature soot oxidation on Pt-Sr/ZrO_2 catalyst,* Master Thesis, Delft University of Technology (2008).

[48] X^{th} Netherlands Catalysis and Chemistry Conference, March 2 - 4, 2009 Noordwijkerhout.

[49] S.-J. Huang, A. B. Walters, and M. A. Vannice, *J. Catal* 192 (2000)**,** 29–47.

[50] E. Xue, K. Seshan, J.R.H. Ross, *Appl. Catal. B: Environ* 11 (1996), 65.
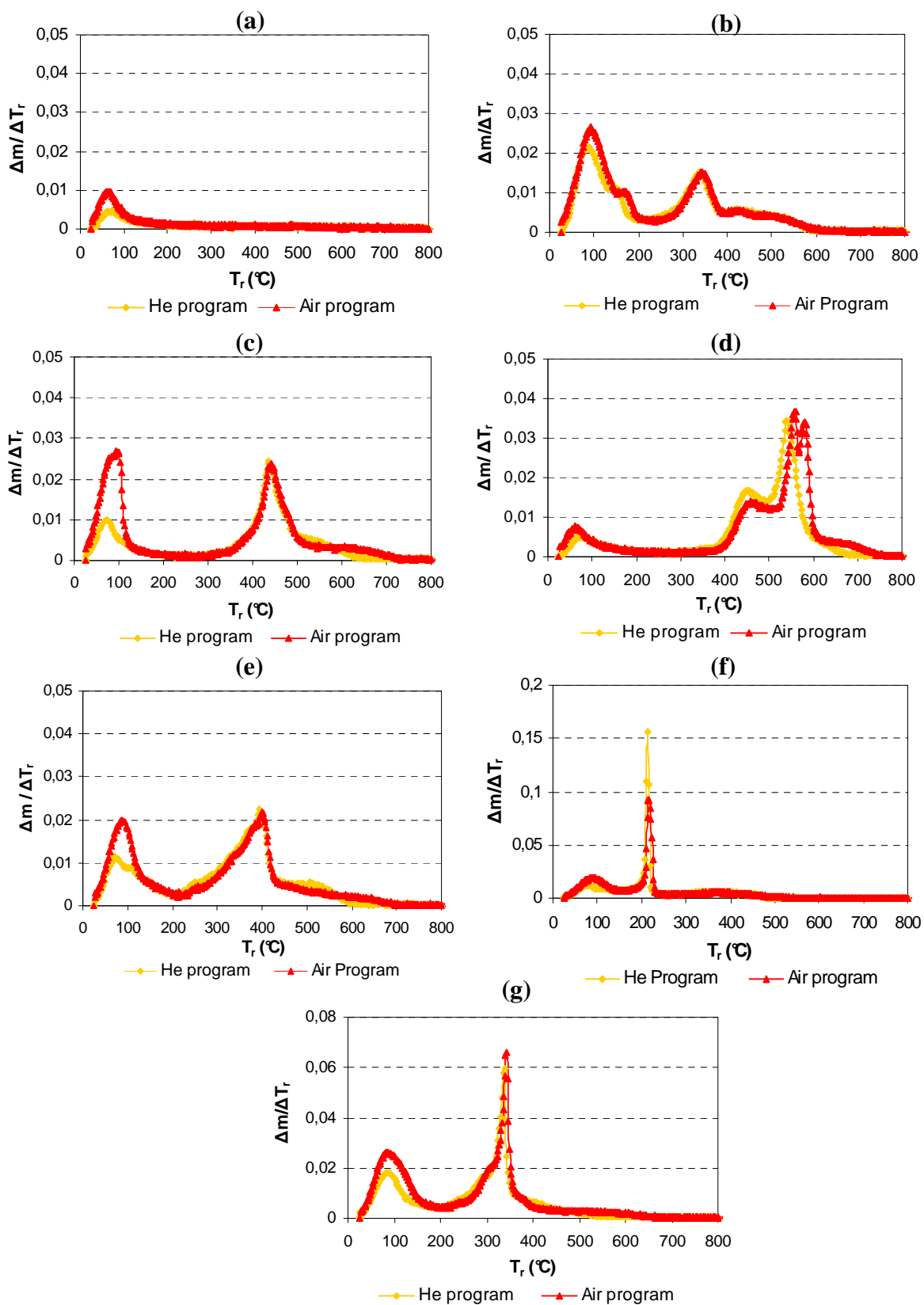
Appendix A – TGA results

Figure A1 - TGA analysis of (a) ZrO_2, (b) $Mg(NO_3)_2/ZrO_2$, (c) $Ca(NO_3)_2/ZrO_2$, (d) $Sr(NO_3)_2/ZrO_2$, (e) $La(NO_3)_3/ZrO_2$, (f) $Ce(NO_3)_3/ZrO_2$ and (g) $Pr(NO_3)_3/ZrO_2$ using Air program and He program. Note: The y axis of graphs (f) and (g) are different than the others.

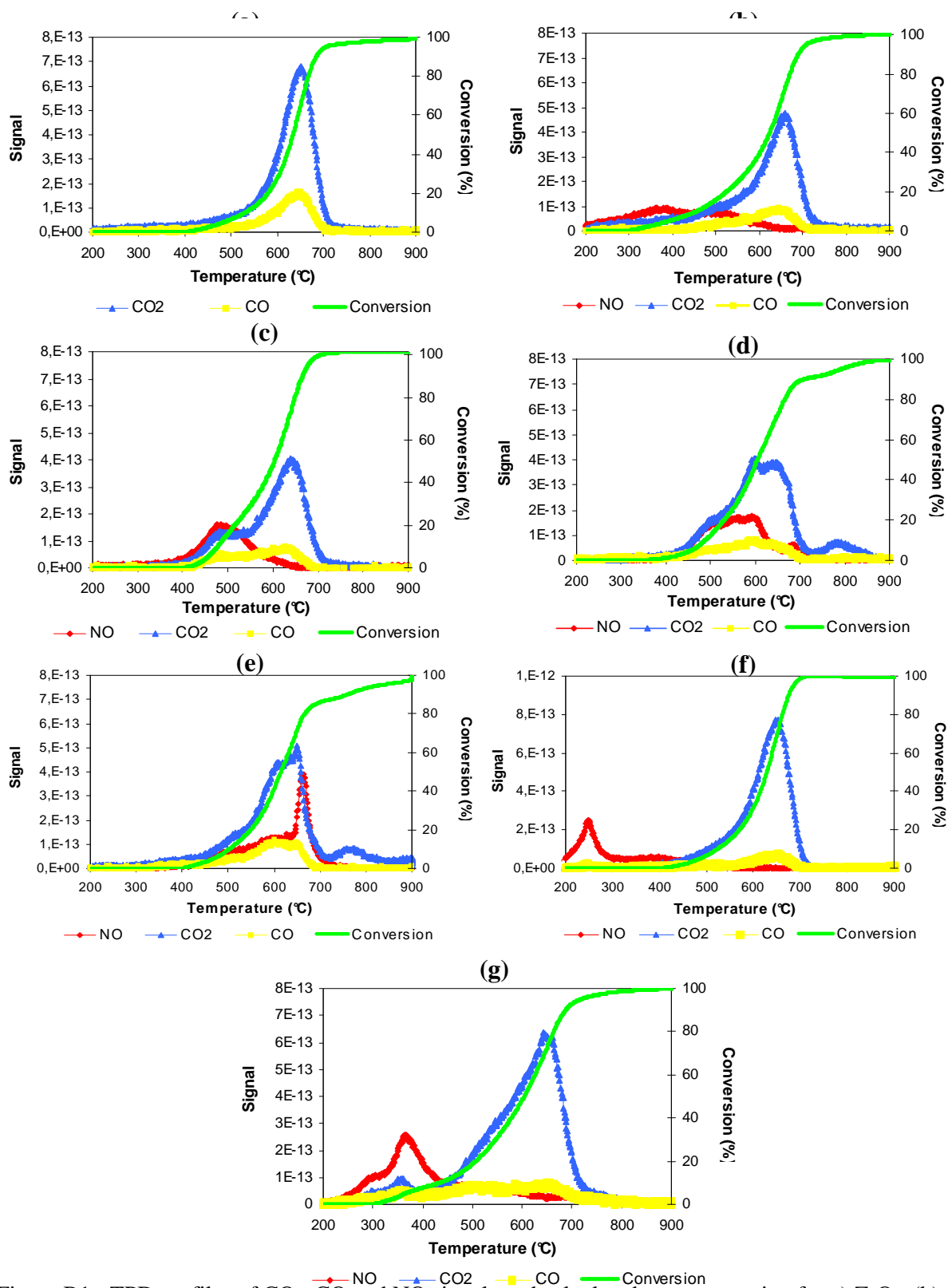# Appendix B

Appendix B1 – TPD-MS Soot Oxidation results

Figure B1 - TPD profiles of CO_2, CO and NO signals and calculated soot conversion for a) ZrO_2, (b) $20\%Mg(NO_3)_2/ZrO_2$, (c) $20\%Ca(NO_3)_2/ZrO_2$, (d) $20\%Sr(NO_3)_2/ZrO_2$, (e) $20\%Ba(NO_3)_2/ZrO_2$, (f) $20\%Ce(NO_3)_3/ZrO_2$ and (g) $20\%Pr(NO_3)_3/ZrO_2$ all of them mixture with soot. Note: The y axis of graph (f) is different than the others.
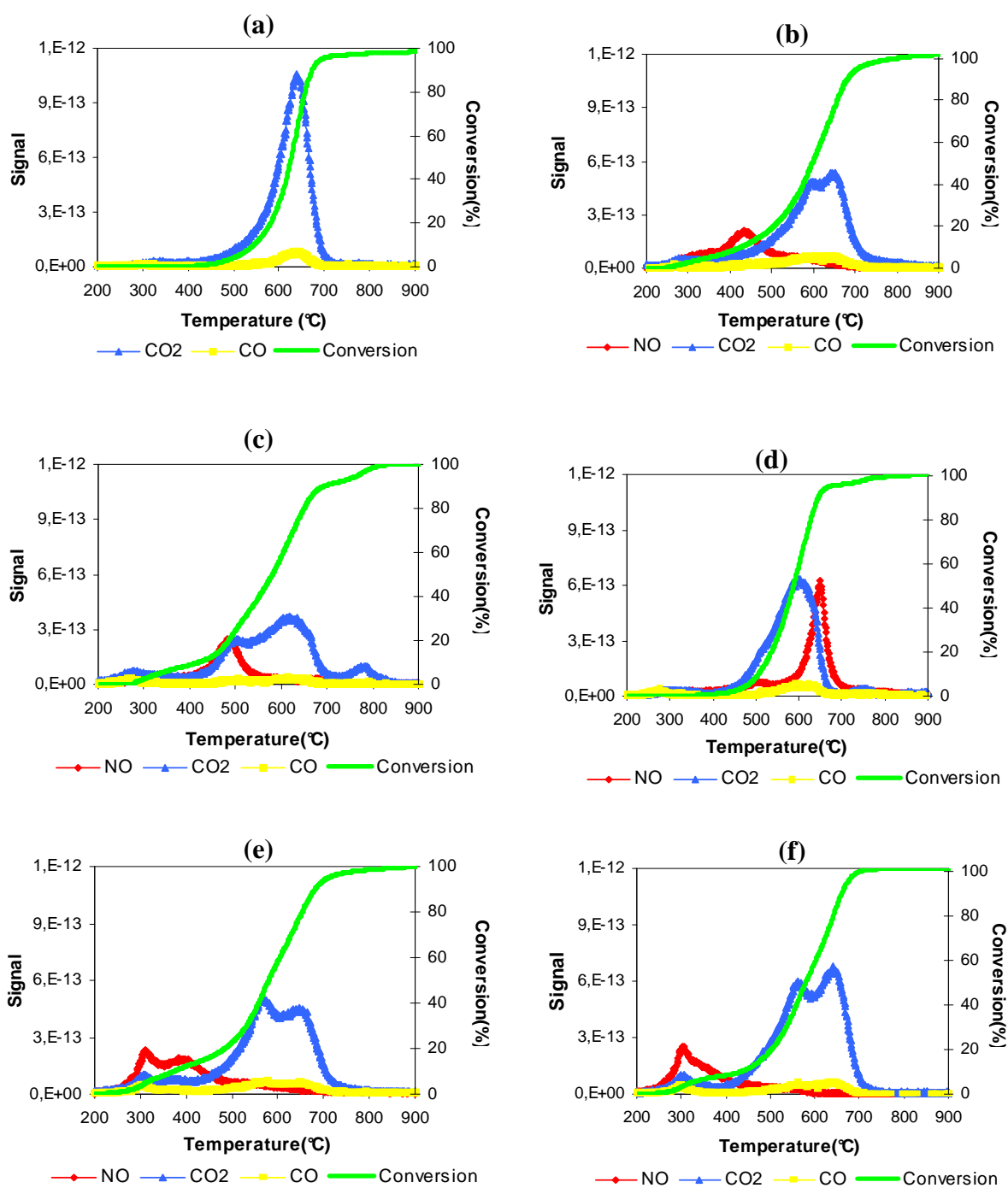
Figure B2 - TPD profiles of CO_2, CO and NO signals and calculated soot conversion for a) $1\%Pt/ZrO_2$, (b) $20\%Ca(NO_3)_2+1\%Pt/ZrO_2$, (c) $20\%Sr(NO_3)_2+1\%Pt/ZrO_2$, (d) $20\%Ba(NO_3)_2+1\%Pt/ZrO_2$, (e) $20\%La(NO_3)_3+1\%Pt/ZrO_2$ and (f) $20\%Pr(NO_3)_3+1\%Pt ZrO_2$ all of them mixture with soot.
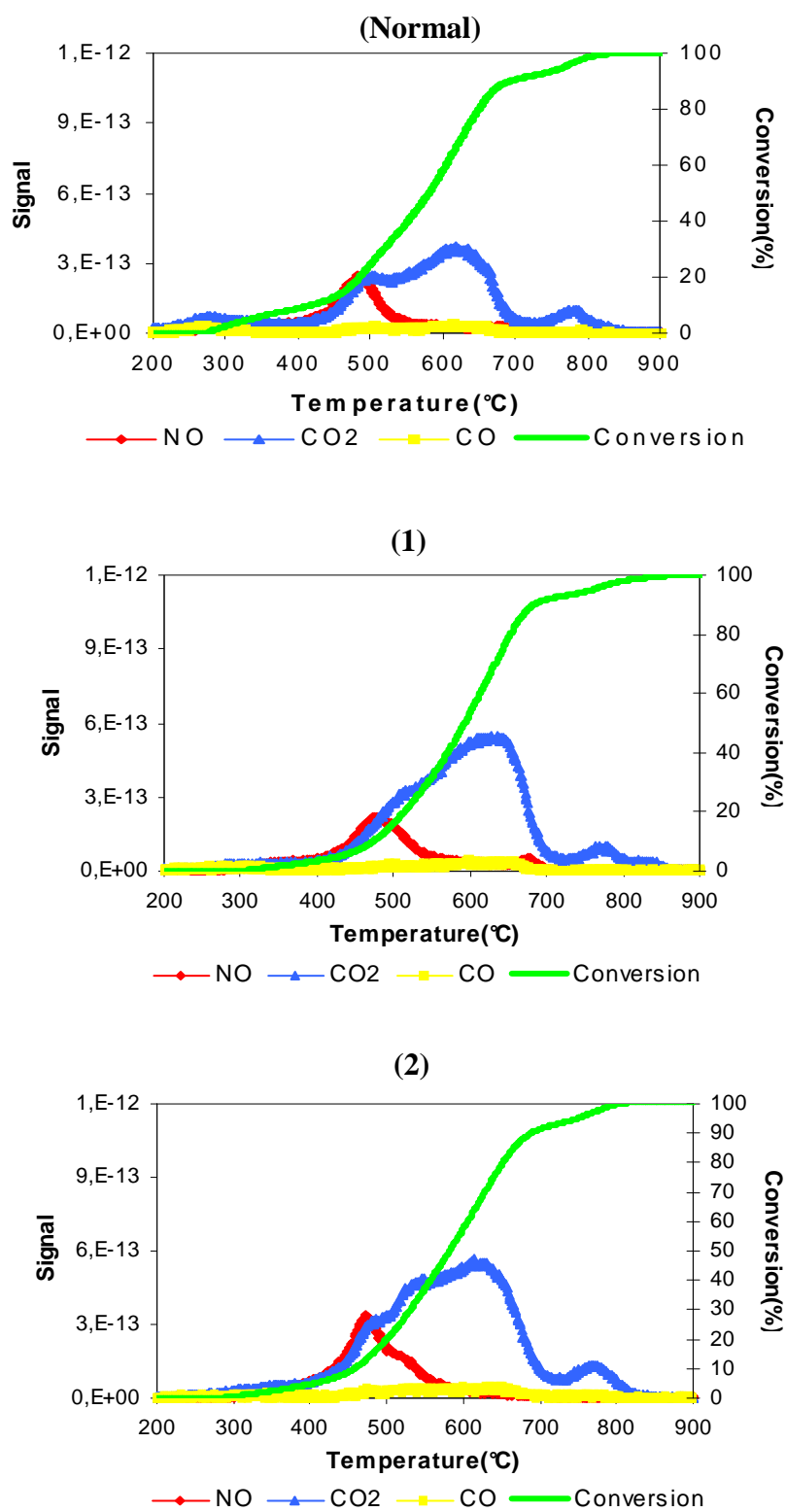
Figure B3 - TPD profiles of CO_2, CO and NO signals and calculated soot conversion for $20\%Sr(NO_3)_2+1\%Pt/ZrO_2$, mixture with soot for the standard, (1) and (2) methods of impregnation.

Appendix B2 – TPD-MS NO$_X$ storage
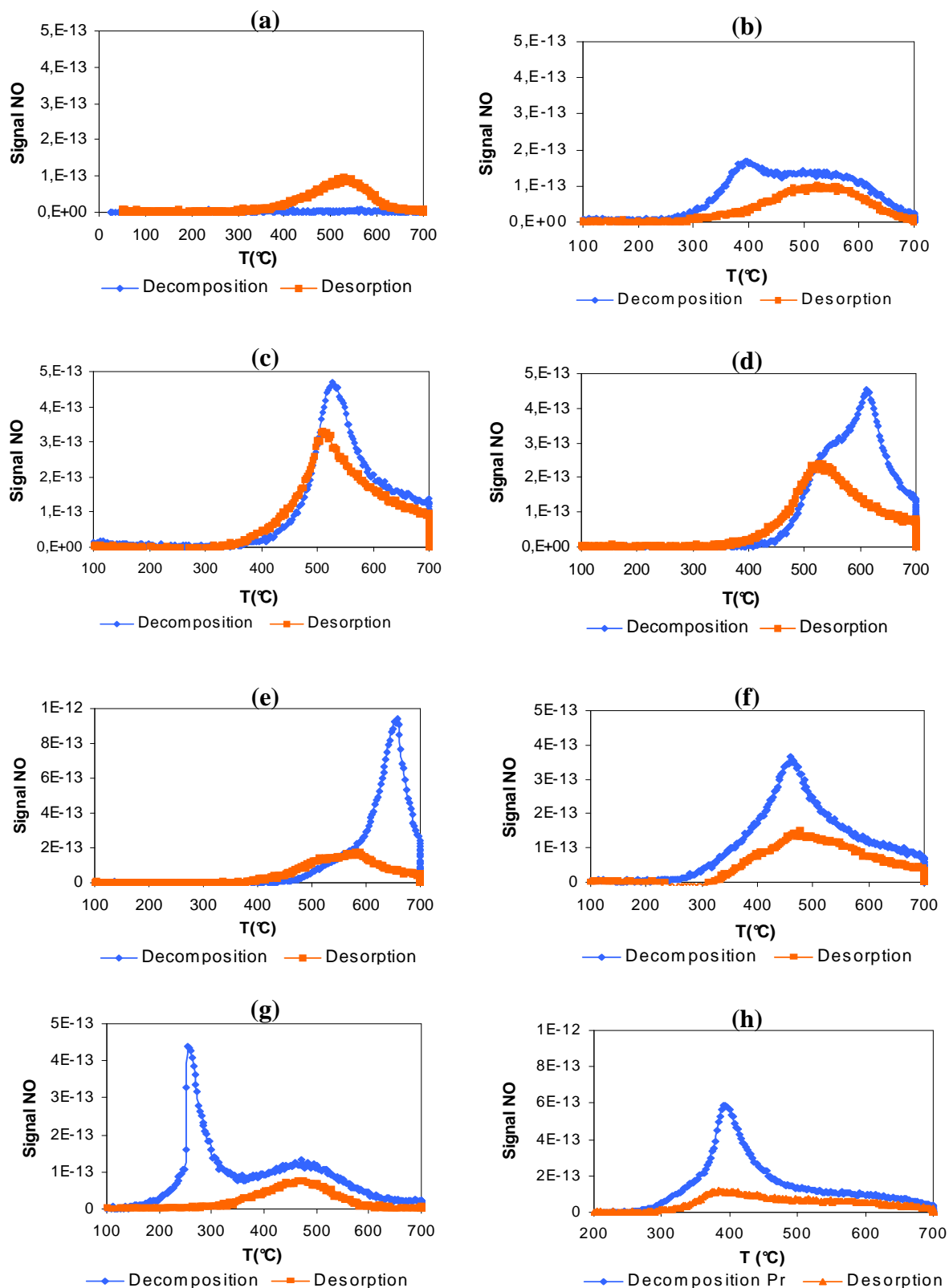
Figure B4 – Decomposition and desorption of nitrates for a) ZrO$_2$,b) 20%Mg(NO$_3$)$_2$ /ZrO$_2$,c) 20%Sr(NO$_3$)$_2$ /ZrO$_2$,d) 20%Ba(NO$_3$)$_2$ /ZrO$_2$,e) 20%La(NO$_3$)$_3$ /ZrO$_2$,f) 20%Ce(NO$_3$)$_3$ /ZrO$_2$,g) 20%Pr(NO$_3$)$_3$ /ZrO$_2$ samples (in a flow of 50 ml/min of air) with increasing of temperature from 25°C to 700°C heating rate of 10°C/min.
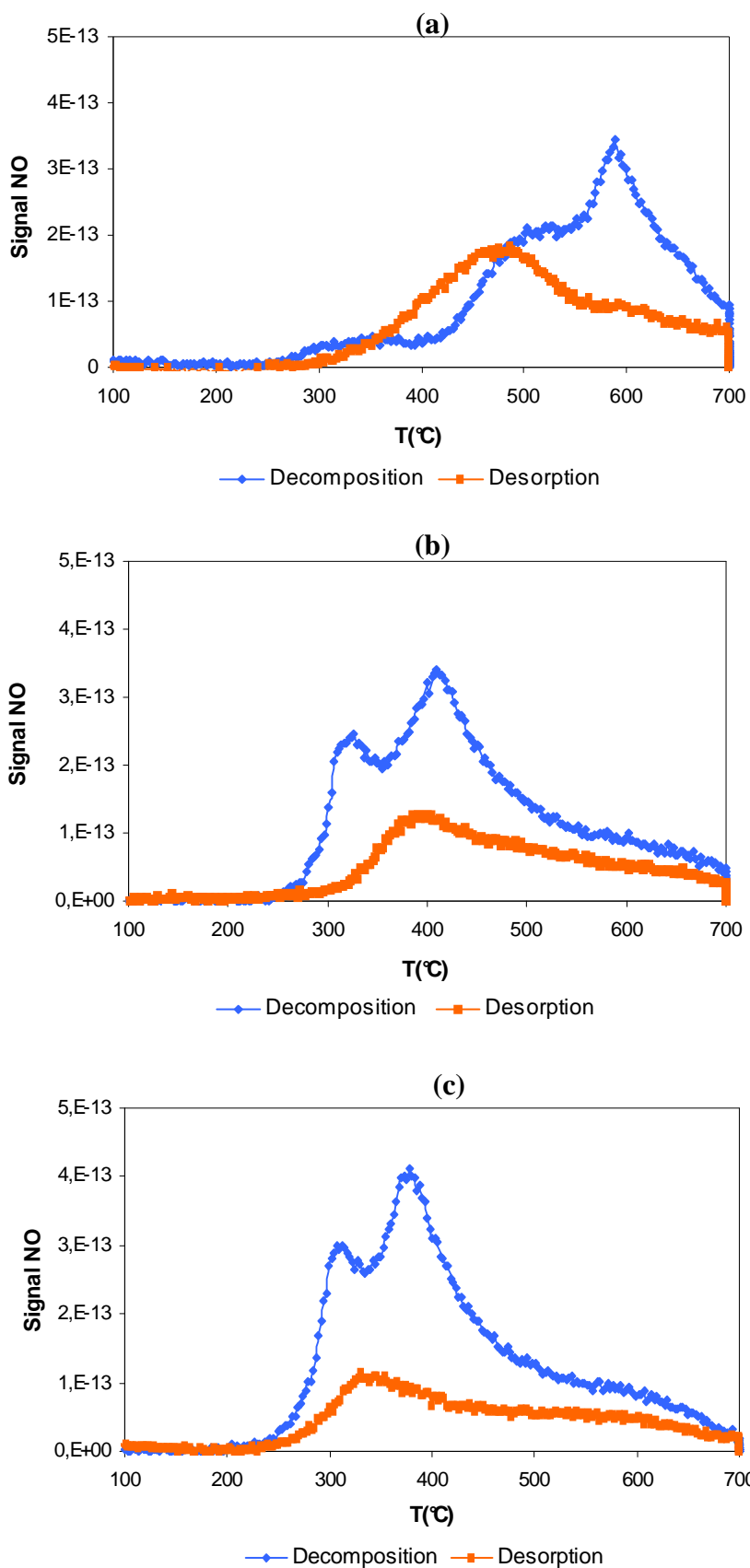
Figure B5 –Decomposition and desorption of nitrates for a) 20%Sr(NO$_3$)$_2$ +1%Pt-ZrO$_2$,b) 20%La(NO$_3$)$_3$ +1%Pt-ZrO$_2$,c) 20%Pr(NO$_3$)$_2$+1%Pt-ZrO$_2$ samples (in a flow of 50 ml/min of air) with increasing of temperature from 25°C to 700°C heating rate of 10°C/min.

Appendix C – Six-flow reactor results

Table C1 - First set of experimental conditions.

Amount of SiC	400	mg
Amount of soot	10	mg
Amount of catalyst	40	mg
P (total pre-pressure)	3.5	bara
P (pressure reactor)	1.1	bara
Flow through reactor	200	ml/min
O_2-Flow	40	ml/min
Ar-Flow	160	ml/min
Temperature programmed:		
20-200 °C	5.0	°C/min
200-600°C	0.5	°C/min
Isotherm on 600°C	20	min
	Catalyst type	
Reactor 1	20% $Sr(NO_3)_2/ZrO_2$	
Reactor 2	20% $Pr(NO_3)_3/ZrO_2$	
Reactor 3	-	
Reactor 4	20% $La(NO_3)_3/ZrO_2$	
Reactor 5	20% $Ba(NO_3)_2/ZrO_2$	
Reactor 6	-	

Figure C1– Soot oxidation in 6-flow reactor: a) 20% $Sr(NO_3)_2/ZrO_2$ b)20% $Pr(NO_3)_3/ZrO_2$,c) 20% $Pr(NO_3)_3/ZrO_2$,d) 20% $Ba(NO_3)_2/ZrO_2$.

Table C2 - Second set of experimental conditions.

Amount of SiC	400	mg
Amount of soot	10	mg
Amount of catalyst	40	mg
P (total pre-pressure)	3.5	bara
P (pressure reactor)	1.1	bara
Flow through reactor	200	ml/min
O_2-Flow	40	ml/min
Ar-Flow	160	ml/min
Temperature programmed:		
20-200 °C	5.0	°C/min
200-600°C	0.5	°C/min
Isotherm on 600°C	20	min
	Catalyst type	
Reactor 1	$20\%Sr(NO_3)_2 + 1\%Pt/ZrO_2$	
Reactor 2	$20\%Pr(NO_3)_3 + 1\%Pt/ZrO_2$	
Reactor 3	-	
Reactor 4	$20\%La(NO_3)_3 + 1\%Pt/ZrO_2$	
Reactor 5	$20\%Ba(NO_3)_2 + 1\%Pt/ZrO_2$	
Reactor 6	-	
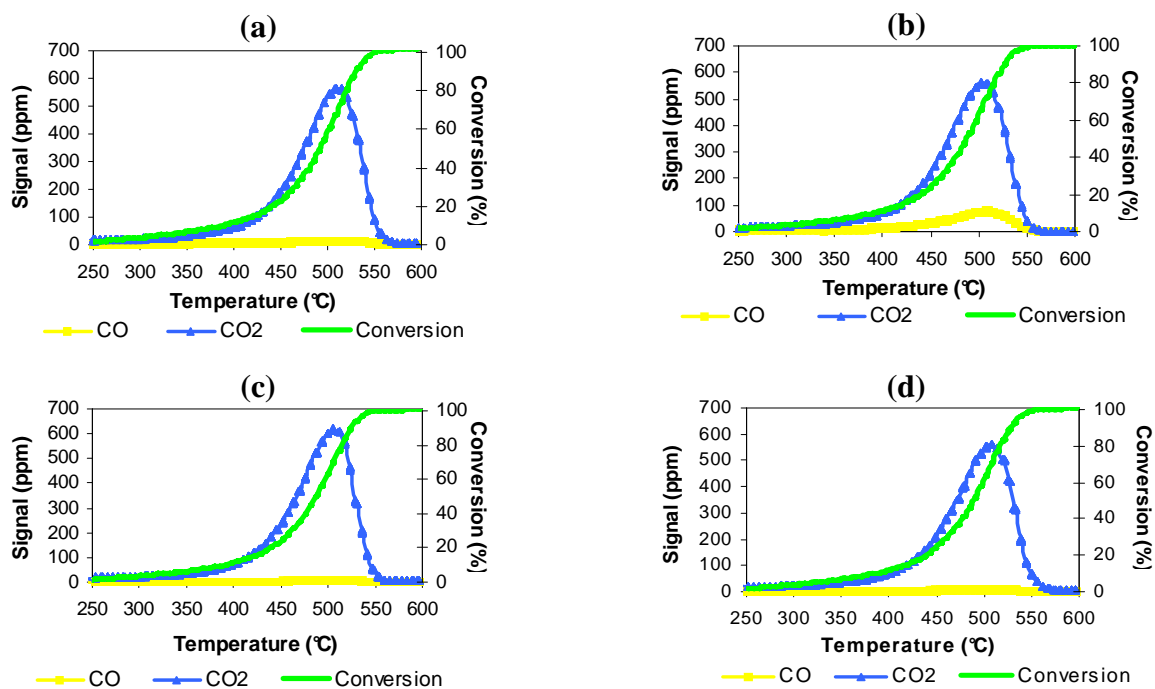
Figure C2 – Soot oxidation in 6-flow reactor: a) $20\%Sr(NO_3)_2+1\%Pt-ZrO_2$, b)$20\%Pr(NO_3)_3+1\%Pt-ZrO_2$,c) $20\%Pr(NO_3)_3+1\%Pt-ZrO_2$,d) $20\%Ba(NO_3)_2+1\%Pt-ZrO_2$.

Table C3 - Third set of experimental conditions.

Amount of SiC	400	mg
Amount of soot	10	mg
Amount of catalyst	40	mg
P (total pre-pressure)	3.5	bara
P (pressure reactor)	1.1	bara
Flow through reactor	200	ml/min
O_2-Flow	40	ml/min
Ar-Flow	160	ml/min

Temperature programmed:

20-200 °C	5.0	°C/min
200-600°C	0.5	°C/min
Isotherm on 600°C	20	min

	Catalyst type
Reactor 1	20%$Ca(NO_3)_2$ /ZrO_2
Reactor 2	20%$Ca(NO_3)_2$+ 1%Pt/ZrO_2
Reactor 3	-
Reactor 4	ZrO_2
Reactor 5	1%Pt/ZrO_2
Reactor 6	-
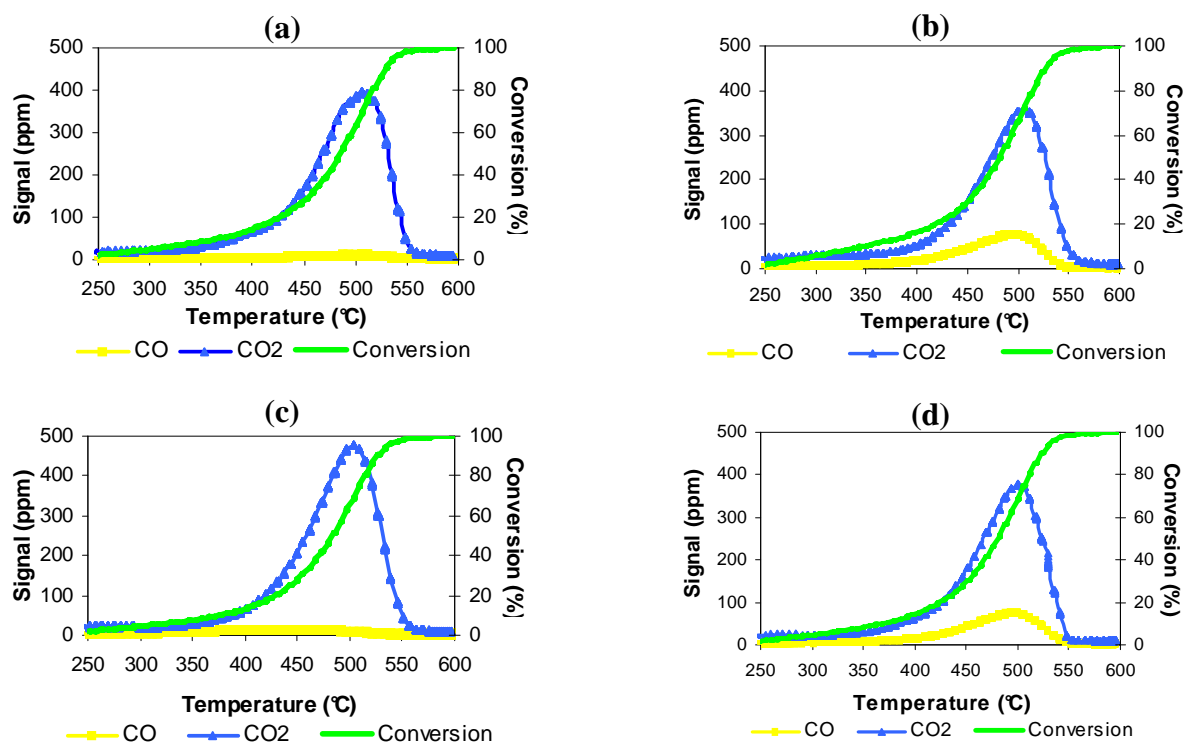
Figure C3 - Soot oxidation in 6-flow reactor: a) 20%$Ca(NO_3)_2$/ZrO_2, b)20%$Ca(NO_3)_2$+1%Pt-ZrO_2 ,c) ZrO_2 ,d) 1%Pt-ZrO_2.

Table C4 - Forth set of experimental conditions.

Amount of SiC	400	mg
Amount of soot	10	mg
Amount of catalyst	40	mg
P (total pre-pressure)	3.5	bara
P (pressure reactor)	1.1	bara
Flow through reactor	200	ml/min
O_2-Flow	40	ml/min
Ar-Flow	160	ml/min
Temperature programmed:		
20-200 °C (in air)	5.0	°C/min
Isotherm at 200°C (in presence of NO)	180	min
200-600°C (in air)	0.5	°C/min
Isotherm on 600°C	20	min
	Catalyst type	
Reactor 1	20% $Sr(NO_3)_2/ZrO_2$	
Reactor 2	20% $Pr(NO_3)_3/ZrO_2$	
Reactor 3	-	
Reactor 4	20% $La(NO_3)_3/ZrO_2$	
Reactor 5	20% $Ba(NO_3)_2/ZrO_2$	
Reactor 6	-	

Figure C4 - Soot oxidation in 6-flow reactor: a) 20% $Ca(NO_3)_2/ZrO_2$, b) 20% $Ca(NO_3)_2+1\%Pt-ZrO_2$,c) ZrO_2 ,d) 1% $Pt-ZrO_2$.

Appendix D – FTIR results

Appendix D1 – Decomposition and desorption of nitrates
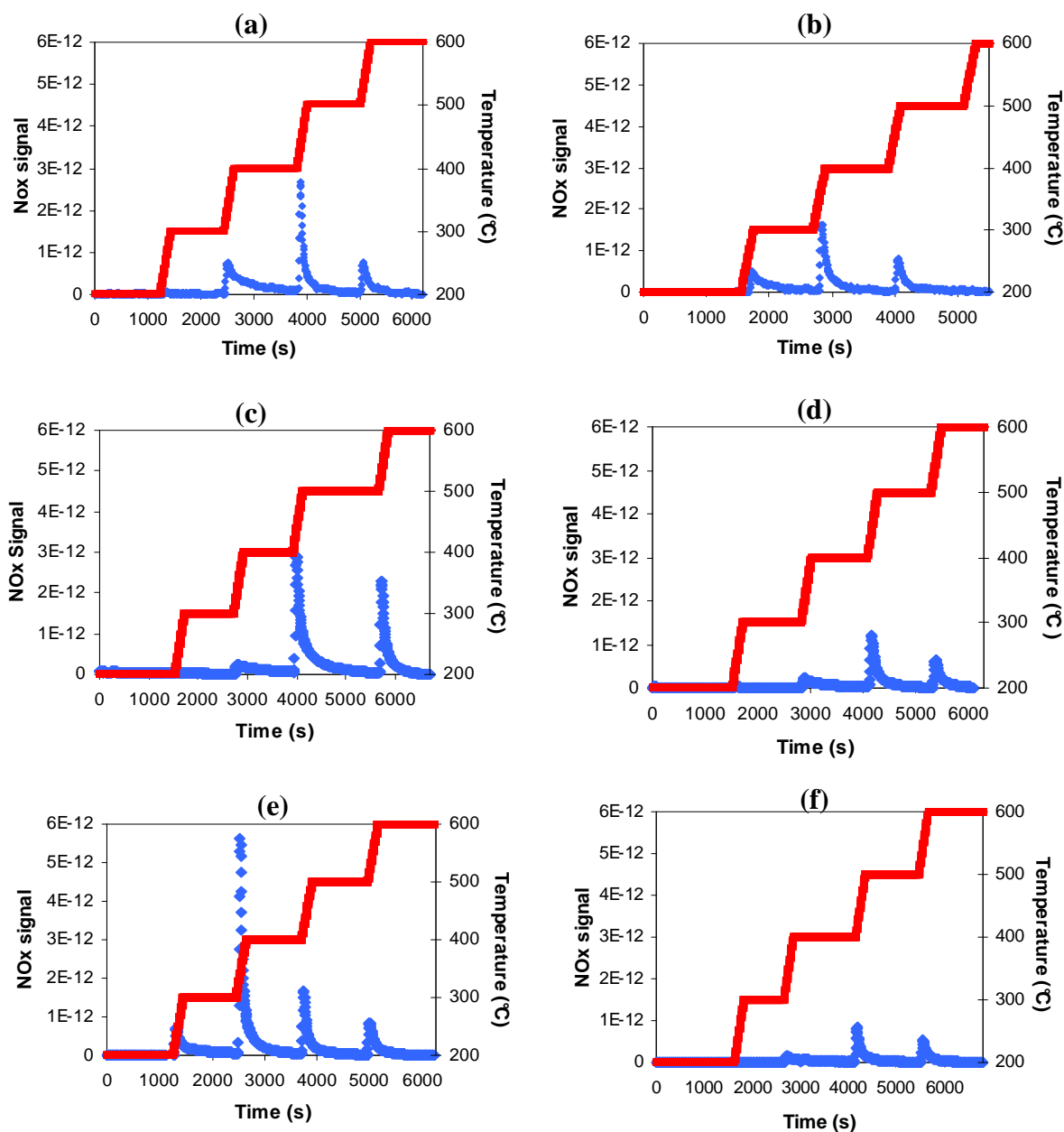
Figure D1 – Decomposition of bulk nitrates a) $20\%Ca(NO_3)_2$ /ZrO_2 c) $20\%Sr(NO_3)_2$/ZrO_2 e) $20\%La(NO_3)_3$ /ZrO_2 (in a flow of 30 ml/min of air) with increasing of temperature from 200°C to 600°C with a 100°C steps, heating rate of 1800°C/h followed by an isotherm of 20 min at each temperature. Desorption b) $20\%Ca(NO_3)_2$ /ZrO_2 d) $20\%Sr(NO_3)_2$/ZrO_2 f) $20\%La(NO_3)_3$ /ZrO_2 (in a flow of 30 ml/min of air) with increasing of temperature from 200°C to 600°C with a 100°C steps, heating rate of 1800°C/h followed by an isotherm of 20 min at each temperature.
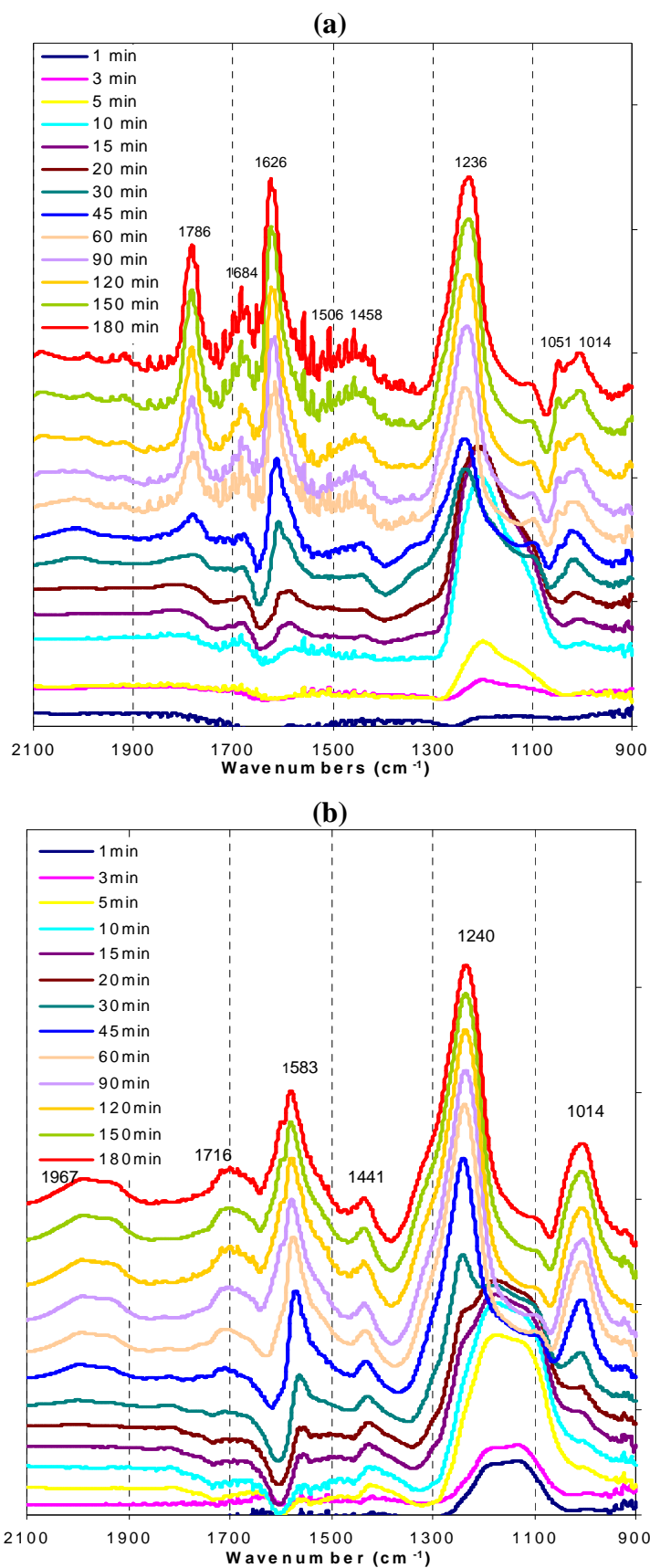
Appendix D2 – Adsorption and Desorption spectra

(a)

(b)

Figure D2 - Adsorption spectra for **a)** 20%SrO/ZrO$_2$; **b)** 20%LaO/ZrO$_2$. Conditions: 800ppm Of NO + 20% of O$_2$ in He at 200°C during 180 minutes.
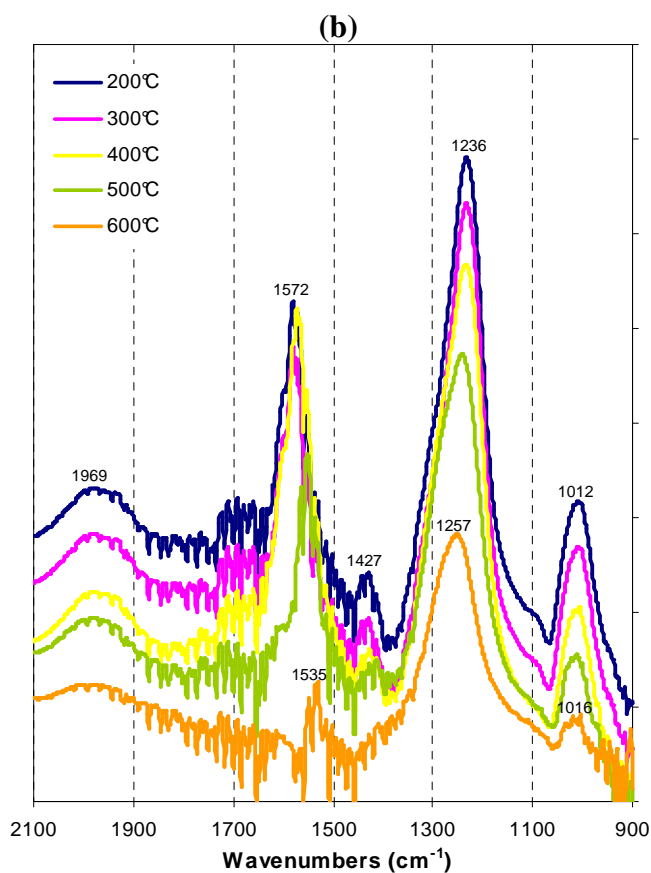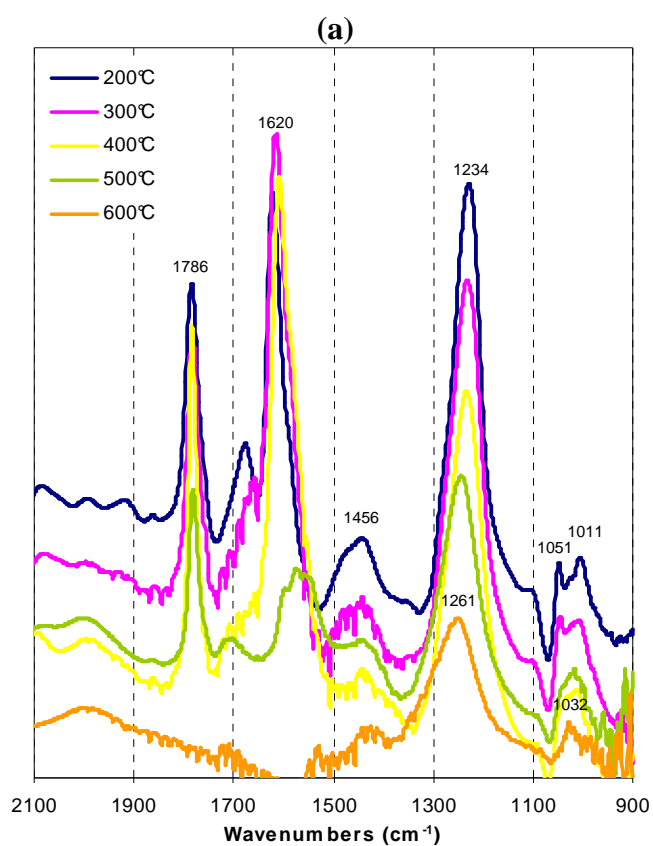
Figure D3 – Desorption spectra for **a)** 20%SrO/ZrO$_2$; **b)** 20%LaO/ZrO$_2$. Conditions: heating rate of 1800°C/h followed by an isotherm of 20 min at each temperature and in a flow of 30 ml/min of air.